

AD~~O~~ 783616

**AFML-TR-74-67**

**THE COLLECTION, GENERATION, AND ANALYSIS OF  
MIL-HDBK-5 ALLOWABLE DESIGN DATA**

*PAUL E. RUFF  
WALTER S. HYLER  
BATTELLE  
COLUMBUS LABORATORIES  
505 KING AVENUE  
COLUMBUS, OHIO 43201*

MAY 1974

ANNUAL REPORT FOR THE PERIOD FEBRUARY 15, 1973 — FEBRUARY 15, 1974

Approved for public release; distribution unlimited.

AIR FORCE MATERIALS LABORATORY  
AIR FORCE SYSTEMS COMMAND  
WRIGHT-PATTERSON AIR FORCE BASE, OHIO 45433

20080820 010

NOTICE

This final report was submitted by Battelle's Columbus Laboratories, 505 King Avenue, Columbus, Ohio 43201, under contract F33615-73-C-5053, job order 73810336, with the Air Force Materials Laboratory, Wright-Patterson Air Force Base, Ohio. Mr. D. A. Shinn (MXA) and Mr. C. L. Harmsworth (MXE) were the laboratory project monitors.

This report has been reviewed and cleared for open publication and/or public release by the appropriate Office of Information (OI) in accordance with AFR 190-17 and DoDD 5230.9. There is no objection to unlimited distribution of this report to the public at large, or by DDC to the National Technical Information Service (NTIS).

This annual report has been reviewed and is approved for publication.

C. L. Harmsworth

C. L. Harmsworth, Technical Manager  
for Engineering and Design Data  
Materials Engineering Branch  
Systems Support Division  
Air Force Materials Laboratory

A. Olevitch

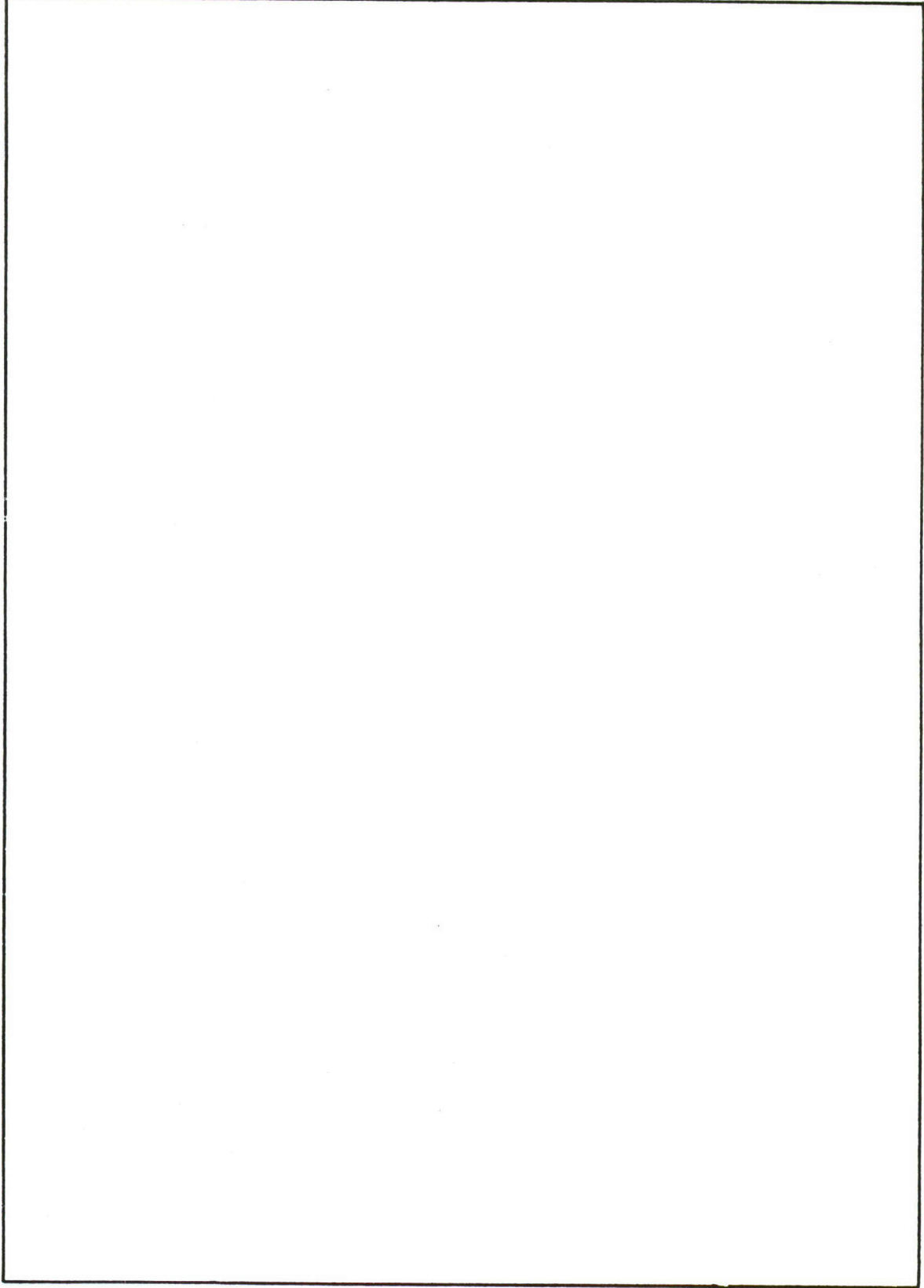
A. Olevitch, Chief  
Materials Engineering Branch  
Systems Support Division  
Air Force Materials Laboratory

Unclassified

SECURITY CLASSIFICATION OF THIS PAGE (When Data Entered)

REPORT DOCUMENTATION PAGE		READ INSTRUCTIONS BEFORE COMPLETING FORM
1. REPORT NUMBER AFML-TR-74-67	2. GOVT ACCESSION NO.	3. RECIPIENT'S CATALOG NUMBER
4. TITLE (and Subtitle) The Collection, Generation, and Analysis of MIL-HDBK-5 Allowable Design Data		5. TYPE OF REPORT & PERIOD COVERED Annual, February 15, 1973 - February 15, 1974
		6. PERFORMING ORG. REPORT NUMBER
7. AUTHOR(s) Paul E. Ruff and Walter S. Hyler		8. CONTRACT OR GRANT NUMBER(s) F33615-73-C-5053
9. PERFORMING ORGANIZATION NAME AND ADDRESS Battelle's Columbus Laboratories 505 King Avenue Columbus, Ohio 43201		10. PROGRAM ELEMENT, PROJECT, TASK AREA & WORK UNIT NUMBERS
11. CONTROLLING OFFICE NAME AND ADDRESS Air Force Materials Laboratory Air Force Systems Command Wright-Patterson Air Force Base, Ohio		12. REPORT DATE May, 1974
		13. NUMBER OF PAGES 63
14. MONITORING AGENCY NAME & ADDRESS (if different from Controlling Office)		15. SECURITY CLASS. (of this report)  Unclassified
		15a. DECLASSIFICATION/DOWNGRADING SCHEDULE
16. DISTRIBUTION STATEMENT (of this Report) Approved for public release; distribution unlimited.		
17. DISTRIBUTION STATEMENT (of the abstract entered in Block 20, if different from Report)		
18. SUPPLEMENTARY NOTES		
19. KEY WORDS (Continue on reverse side if necessary and identify by block number)		
aluminum castings	physical properties	
fasteners	plain-strain fracture toughness	
fatigue	plain-stress fracture toughness	
fatigue-crack-propagation	stress corrosion	
	stress-strain curves	
20. ABSTRACT (Continue on reverse side if necessary and identify by block number)		
<p>This annual report describes highlights of some of the work performed by Battelle's Columbus Laboratories, a contractor to the Air Force Materials Laboratory, to update MIL-HDBK-5. Included is a description of work performed in the areas of fatigue, fatigue-crack-propagation, plain-strain fracture toughness, plane-stress fracture toughness, stress corrosion, fasteners, design allowable properties for aluminum castings, stress-strain curves, and physical properties.</p>		

SECURITY CLASSIFICATION OF THIS PAGE(When Data Entered)



SECURITY CLASSIFICATION OF THIS PAGE(When Data Entered)

AD783616

## SUMMARY

Since the previous annual reports delineated the functional activities and services provided by BCL personnel for the MIL-HDBK-5 program, this report describes briefly some of the more important technical activities.

A fatigue data consolidation and statistical analysis procedure was developed by BCL personnel during the past several years, which can be applied to constant amplitude, uniaxial fatigue data to provide a measure of fatigue data variability and probability of survival. With this procedure, fatigue data from different stress ratios (or mean stresses) and notch concentrations can be consolidated and statistically analyzed. The method of analysis was tested on collections of fatigue data for 2024 and 7075 aluminum alloys, Ti-6Al-4V alloy, and 300M steel with generally good results. Guidelines, delineating this newly developed analytical technique and the method of presenting fatigue data in MIL-HDBK-5B, will be proposed to the MIL-HDBK-5 Coordination Activity for approval at the April 23-25, 1974 meeting.

Research conducted by BCL personnel has involved formulating methods for the analysis of fatigue-crack-propagation data. The crack-growth model developed allows the consolidation and representation of data from tests conducted at different stress ratios for a given material. The model has been fitted to aluminum, steel, and titanium alloys to produce empirical formulas and statistical results characterizing the crack-growth behavior of the materials. Very satisfactory representation of the data was obtained in most cases. Preliminary guidelines delineating this newly developed analytical technique and the method of presenting fatigue-crack-propagation data in MIL-HDBK-5B will be presented to the MIL-HDBK-5 Coordination Activity for discussion at the April 23-25, 1974 meeting.

Guidelines describing the analytical technique and the method of presenting plane-strain fracture toughness data have been included in Chapter 9 of MIL-HDBK-5B. Some  $K_{Ic}$  data for a few alloys have been added to the Handbook. Due to the limited quantity of data available, these values are based upon simple averages and are designated "for information only". Current efforts are directed to the collection of additional plane-strain fracture data as well as data for other alloys. The goal is to obtain statistically significant quantities of fracture data so that this property can be

incorporated into the Handbook on a statistical (A and B) basis similar to other design allowables.

Guidelines describing the analytical technique and the method of presenting plane-stress fracture data were approved at the 44th meeting and will appear in Change Notice 2. A proposal containing six displays of residual strength data for 7075 aluminum alloy were approved at the 46th meeting and these data will appear in Change Notice 3. Current efforts are directed to the collection and analysis of additional plane-stress data.

An analytical procedure has been developed for the determination of statistically based design allowable properties (A and B values) for aluminum casting alloys. Current efforts involve the collection of A-357 tensile data from production castings. If a statistically significant quantity of appropriately documented A-357 data can be obtained, these observations can be used to verify the newly developed analytical method.

In the area of fasteners, considerable effort has been expended in the revision of Section 9.4.1, "Guidelines for Presentation of Data for Mechanically Fastened Joints". The proposed revision will include (1) new 0.04D yield criteria, (2) method for the analysis of flush-head fasteners whose heads penetrate the second sheet, (3) data requirements and analysis methods for limited quantities of data not intended for inclusion in MIL-HDBK-5B, (4) graphical presentation formats and methods of analysis of static joint data, (5) sponsor and reporting requirements for new fasteners, and (6) a standard failure code. The final draft of this proposed revision will be presented to the MIL-HDBK-5 Coordination Activity for approval at the 47th meeting on April 23-25, 1974. A plan has been devised to implement a complete revision of Chapter 8.

An investigation revealed that meaningful stress corrosion data cannot be incorporated into MIL-HDBK-5B until standardized test procedures for stress corrosion testing have been established. The American Society for Testing Materials (ASTM) is actively involved issuing such standards. The ASTM progress will continue to be monitored by the MIL-HDBK-5 Coordination Activity until all of these standards are published.

A MIL-HDBK-5 testing program is currently in progress. The objective is to perform the necessary tests required to provide missing design properties in MIL-HDBK-5B. Tests are being conducted on five materials:

(1) 9Ni-4Co-.20C plate, (2) Ti-6Al-6V-2Sn annealed extrusions, (3) 17-4PH (H1025 and H1150) bar, (4) 15-5PH (H1025 and H1150) bar, and (5) 2024-T86 sheet.

As a result of a revision of the Guidelines Section 9.3.2, "Typical Stress-Strain and Stress-Tangent Modulus Curves", which was incorporated in Change Notice 1, new requirements for stress-strain curves were established. This necessitated the updating of stress-strain curves in MIL-HDBK-5B. This task is currently under way. In addition, more emphasis has been placed in the incorporation of stress-strain curves in the Handbook.

Section 9.1.6, "Requirements for New Materials" was added to Chapter 9, "Guidelines for the Presentation of Data", in Change Notice 1 to MIL-HDBK-5B. The purpose of these guidelines was to establish minimum data requirements for new materials to be considered for inclusion in MIL-HDBK-5B.

Efforts are currently under way to update the physical properties in MIL-HDBK-5B. A considerable quantity of additional physical property data for some alloys has been generated since the physical property values were incorporated in the Handbook. Agenda Item 72-23, Coefficient of Thermal Expansion for Ti-6Al-4V, approved at the 45th meeting, and Item 73-8, Physical Property Data for Titanium Alloys, approved at the 46th meeting, have completed the update for the titanium chapter. Agenda Item 73-20, Physical Properties of Nickel Base Alloys, will be considered for approval by the MIL-HDBK-5 Coordination Activity at the 47th meeting in April, 1974.

Change Notice 1, dated July 1, 1972, which incorporated the changes and additions approved at the 42nd and 43rd meetings, was issued in February, 1973. Change Notice 2, dated August 31, 1973, which included the changes and additions approved at the 44th and 45th meetings, is in the process of being printed and should be available in May, 1974.

## PREFACE

The authors wish to gratefully acknowledge the contributions made to this report by the following Battelle personnel: C. E. Feddersen, R. J. Favor, R. Rice, S. Ford, and K. Davies.

## LIST OF CONTENTS

	<u>Page</u>
INTRODUCTION . . . . .	7
FATIGUE . . . . .	8
FATIGUE-CRACK PROPAGATION . . . . .	19
FRACTURE TOUGHNESS . . . . .	30
STRESS CORROSION . . . . .	37
CASTING DESIGN DATA . . . . .	38
FASTENERS . . . . .	41
REQUIREMENTS FOR NEW MATERIALS . . . . .	42
PHYSICAL PROPERTIES . . . . .	45
STRESS-STRAIN AND STRESS-TANGENT MODULUS CURVES . . . . .	49
MIL-HDBK-5B REVISIONS . . . . .	53
MIL-HDBK-5 TEST PROGRAM . . . . .	53
APPENDIX A — STATISTICAL METHODS OF ANALYSIS . . . . .	55
REFERENCES . . . . .	58
SYMBOLS . . . . .	61

## LIST OF ILLUSTRATIONS

	<u>Page</u>
Figure 1. Schematic illustration of regressed inverse hyperbolic tangent curve and appropriate functional limits . . . . .	12
Figure 2. Consolidated 2024-T3 sheet data (unnotched) with fitted mean curves and 90 and 99 percent probability of survival lines . . . . .	13
Figure 3. Consolidated 2024-T3 sheet data (notched) with fitted mean curve and 90 and 99 percent probability of survival lines. . . . .	13
Figure 4. Consolidated 7075-T6 sheet data (unnotched) with fitted mean curve and 90 and 99 percent probability of survival lines . . . . .	14
Figure 5. Consolidated 7075-T6 sheet data (notched) with fitted mean curve and 90 and 99 percent probability of survival lines. . . . .	14
Figure 6. Consolidated 300M billet and forging data (unnotched) with fitted mean curve and 90 and 99 percent probability of survival lines . . . . .	15
Figure 7. Consolidated 300M billet and forging data (notched) with fitted mean curve and 90 and 99 percent probability of survival lines . . . . .	15

LIST OF ILLUSTRATIONS (Continued)

		<u>Page</u>
Figure 8.	Consolidated STA Ti-6Al-4V sheet data (unnotched) with fitted mean curve and 90 and 99 percent probability of survival lines . . . . .	16
Figure 9.	Consolidated STA Ti-6Al-4V sheet data (notched) with fitted mean curve and 90 and 99 percent probability of survival lines . . . . .	16
Figure 10.	Presentation of fatigue-crack-growth data . . . . .	20
Figure 11.	Fatigue-crack-propagation-rate curve for 2024-T3 aluminum alloy . . . . .	25
Figure 12.	Fatigue-crack-propagation-rate curve for 7075-T6 aluminum alloy . . . . .	26
Figure 13.	Fatigue-crack-propagation-rate curve for 7075-T7351 aluminum alloy . . . . .	27
Figure 14.	Fatigue-crack-propagation curve for 300M steel . . . . .	28
Figure 15.	Fatigue-crack-propagation-rate curve for Ti-6Al-4V alloy . . . . .	29
Figure 16.	Typical load-compliance record of a structural component containing a flaw . . . . .	32
Figure 17.	Variation of fracture toughness with thickness or stress state (size effect) . . . . .	34
Figure 18.	Crack growth curve . . . . .	36
Figure 19.	Working curve showing effect of temperature on the specific heat of commercially pure titanium . . . . .	47
Figure 20.	Working curve showing effect of temperature on the thermal expansion of commercially pure titanium . . . . .	47
Figure 21.	Working curve showing effect of temperature on the thermal conductivity of commercially pure titanium . . . . .	48
Figure 22.	Effect of temperature on the physical properties of commercially pure titanium . . . . .	48
Figure 23.	Typical tensile stress-strain curves at room temperature for various heat treated conditions of 15-5PH stainless steel bar . . . . .	51
Figure 24.	Typical tensile stress-strain curves for annealed Inconel Alloy 625 sheet at room and elevated temperatures . . . . .	51
Figure 25.	Typical compressive stress-strain and tangent modulus curves for annealed Inconel Alloy 626 sheet at room and elevated temperatures . . . . .	52

THE COLLECTION, GENERATION, AND ANALYSIS  
OF MIL-HDBK-5 ALLOWABLE DESIGN DATA

by

Paul E. Ruff and Walter S. Hyler

INTRODUCTION

This annual report describes highlights of the activities, accomplishments, and progress of the MIL-HDBK-5 program from February 15, 1973, through February 15, 1974. The Military Standardization Handbook, MIL-HDBK-5B, "Metallic Materials and Elements for Aerospace Vehicle Structures", is recognized as the primary source for design allowable data by the Department of Defense (DoD) and other Government agencies responsible for aerospace vehicle design. The Handbook contains design allowable data on metallic materials, fasteners, joints, and other structural elements. The maintenance of this document is achieved through the cooperative efforts of the Air Force, Navy, Army, Federal Aviation Agency (FAA), National Aeronautics and Space Administration (NASA), and industrial users and suppliers of metallic aerospace materials. The DoD has designated the Air Force as the activity responsible for preparing this Handbook. As such, the Air Force Materials Laboratory (AFML) has contracted with Battelle's Columbus Laboratories (BCL) to provide the planning, coordination, and implementation necessary to develop and maintain current design allowable data and other related information in MIL-HDBK-5.

The previous annual reports<sup>(1,2)</sup> described in detail the functional activities performed by BCL. Since the functional activities are somewhat repetitive from year to year, this report briefly describes some of the more important MIL-HDBK-5 technical activities. Because of the complexity of

- 
- (1) Ruff, Paul E., Favor, Ronald J., and Hyler, Walter S., "The Collection, Generation, and Analysis of MIL-HDBK-5 Allowable Design Data", AFML-TR-72-61 (March, 1972).
  - (2) Ruff, Paul E., Favor, Ronald J., and Hyler, Walter S., "The Collection, Generation, and Analysis of MIL-HDBK-5 Allowable Design Data", AFML-TR-73-79 (March, 1973).

these activities, these summaries are not restricted to work accomplished only during the reporting period. Some items which are not technical in nature have been included for informational purposes. The technical effort involved in statistical analyses and the determination of design allowables in accordance with the guidelines in Chapter 9 of MIL-HDBK-5B have not been included since this work has been reported previously in the agenda and minutes for the 45th and 46th MIL-HDBK-5 Coordination Meetings.

During the reporting period, AFML, FAA, and Army Materials and Mechanics Research Center provided funds to support the MIL-HDBK-5 program.

## FATIGUE

Metal fatigue is a critical factor in the design of aerospace structures, and it is important to analyze and present available constant-amplitude fatigue data, both high and low cycle, in a manner which provides information of maximum usefulness in the establishment of appropriate design stress levels. All fatigue data currently presented in MIL-HDBK-5B represent relatively long life conditions ( $> 10^4$  cycles to failure) and are displayed either in terms of stress versus number of cycles to failure (S-N) curves or in the form of constant life (modified Goodman) diagrams. Such curves and diagrams are based on typical or average values of fatigue life and have no statistical basis; they merely reflect average data trends and provide no information regarding data scatter or probability of survival of a particular material under a given set of loading conditions.

A fatigue data consolidation and statistical analysis procedure was developed by BCL personnel during the past several years, which can be applied to constant-amplitude, uniaxial fatigue data to provide a measure of fatigue data variability and probability of survival. With this procedure, fatigue data from different stress ratios (or mean stresses) and notch concentrations can be consolidated and statistically analyzed. The method of analysis was tested on collections of fatigue data for 2024 and 7075 aluminum alloys, Ti-6Al-4V alloy, and 300M steel with generally good results. An outline of the analytical procedure and selected results are presented in the following

sections. For a more detailed discussion of the background work, see References (3) and (4).

Guidelines, delineating this newly developed analytical technique and the method of presenting fatigue data in MIL-HDBK-5B, are being prepared and will be proposed to the MIL-HDBK-5 Coordination Activity for approval at the April 23-25, 1974 meeting.

#### Development of Analytical Methods

An examination of available constant-amplitude fatigue data showed that most often there are insufficient data to perform a reasonable statistical analysis on a given S-N curve at a particular value of mean stress (or stress ratio) or at a certain notch concentration factor. In an attempt to alleviate this problem, several methods were investigated which would potentially allow a combination of data for various mean stresses or notch concentrations.

Consolidation of Unnotched Data - An equivalent strain parameter was used in the analysis of smooth specimen fatigue data to account for the effects of mean stress or stress ratio. The formulation used is similar in form to the parameter proposed by Walker<sup>(5)</sup>. It is defined in terms of a multiplicative combination of strain range and maximum stress:

$$\epsilon_{eq} = (2\epsilon_a)^m (S_{max}/E)^{1-m} \quad (1)$$

where m represents a constant to be optimized for a particular material. (Symbols are defined on pages 61 through 63.)

To define an equivalent strain in cases where strain was not measured or controlled, it was necessary to calculate values of  $\epsilon_a$ . The cyclically stable stress-strain curve was used to estimate values of  $\epsilon_a$  from known values of  $\sigma_a$ . For all the materials considered in this study, it was found that this curve could be well approximated by a trilinear function defined as follows:

- (3) Jaske, C. E., Feddersen, C. E., Davies, K. B., and Rice, R. C., "Analysis of Fatigue, Fatigue-Crack Propagation, and Fracture Data", Final Report to NASA-Langley Research Center, NASA CR-132332 (November, 1973).
- (4) Rice, R. C., and Jaske, C. E., "Consolidated Presentation of Fatigue Data for Design Applications", presented at the 1974 SAE Automotive Engineering Congress and Exposition, Detroit, Michigan (February, 1974).
- (5) Walker, K., "The Effect of Stress Ratio During Crack Propagation and Fatigue for 2024-T3 and 7075-T6 Aluminum", Effects of Environment and Complex Load History on Fatigue Life, STP 462, ASTM (1970), pp 1-14.

$$\sigma_a = E\epsilon_a, \quad 0 \leq \sigma_a \quad (1)$$

$$\sigma_a = K_1 \epsilon_a^{n_1}, \quad \sigma_a(1) < \sigma_a \leq \sigma_a(2) \quad (2)$$

$$\sigma_a = K_2 \epsilon_a^{n_2}, \quad \sigma_a > \sigma_a(2) \quad .$$

Using Equation (2), values of  $\epsilon_{eq}$  were calculated for each data set and specific values of the constant  $m$ . A third order polynomial was then fit to the data through a least squares regression process so that the optimum  $m$  value could be selected. Fatigue life was treated as the dependent variable and equivalent strain was considered the independent variable, with the resultant expression being:

$$\log N_f = A_0 + A_1 \epsilon_{eq} + A_2 \epsilon_{eq}^2 + A_3 \epsilon_{eq}^3 \quad . \quad (3)$$

Through determination of the statistical parameter,  $R^2$  (see Appendix A), the degree of data collapse (i.e., the "correctness" of the  $m$  value) was quantitatively measured.

Results of this analysis revealed that it was possible to define a single value of  $m$  for all the investigated materials. Definition of equivalent strains with an  $m$  value of 0.40 resulted in nearly maximum consolidations of data for the aluminum, titanium, and steel alloys.

Consolidation of Notched Data - In the notched analysis, the equivalent strain parameter, with  $m = 0.40$ , was again used as a means of data consolidation; the only difference in analysis being that estimates of local stress and strain were used in place of nominal values.

Cyclic plastic deformation at the notch root can cause localized cyclic hardening or softening of the material, so estimates of local strain amplitude were calculated by using a cyclic stress-strain curve in combination with nominal values modified by a fatigue-strength reduction factor<sup>(6)</sup>. The resultant approximation of local strain was given by:

$$\epsilon_a = K_f \epsilon_a \quad , \quad (4)$$

where

$$K_f = 1 + \frac{K_t - 1}{1 + \rho/r} \quad . \quad (5)$$

Because of potential cyclic relaxation of mean stress, it was not possible to compute local values of maximum stress directly from nominal

(6) Metal Fatigue, Edited by G. Sines and J. L. Waisman, McGraw-Hill Book Company (1959), "Notch-Sensitivity" (R. E. Peterson), pp 293-306.

values. Instead, it was found that the best results were obtained when the local mean stress was related to monotonic values

$$\sigma_m = \sigma'_{\max} - f_m(\epsilon_a') \quad , \quad (6)$$

and the local stress amplitude was related [from Equation (4)] to the cyclic stress-strain curve

$$\sigma_a = f_c(\epsilon_a) \quad , \quad (7)$$

so that, combining Equations (6) and (7), the local maximum stress was approximated by

$$\sigma_{\max} = f_c(\epsilon_a) + \sigma'_{\max} - f_m(\epsilon_a') \quad . \quad (8)$$

This empirical relationship was found to work well for constant-amplitude loading where most of the cyclic life was at the stable relaxed mean stress.

Optimum values of  $\rho$  for Equation (5) were found to vary considerably from material to material. Maximum consolidation of data for the two aluminum alloys was obtained when  $\rho$  was approximately 0.007 inch; a  $\rho$  value of 0.0018 inch was found for the 300M steel and a value of 0.0008 inch was determined on a sample of Ti-6Al-4V bar data.

Relationship Between Equivalent Strain and Fatigue Life - After methods of consolidating notched and unnotched data had been developed, efforts were directed toward the establishment of a continuous analytical function which would accurately describe the mean trends of the consolidated data.

After reviewing a variety of functions, it was found that the inverse hyperbolic tangent function provided a reasonable model of fatigue data trends ranging from 10 to 10<sup>8</sup> cycles to failure. This function can be expressed in terms of a transformed linear regression equation of the form

$$Y = A_0 + A_1 \tanh^{-1} \left[ \frac{\log(\epsilon_u \epsilon_e / \epsilon_{eq}^2)}{\log(\epsilon_u \epsilon_e)} \right] \quad . \quad (9)$$

Values of  $\epsilon_u$  and  $\epsilon_e$  were selected to appropriately bound the complete range of data as illustrated in Figure 1. In the overall data analysis optimum values of  $\epsilon_u$  varied from 0.015 to 0.017 and best values of  $\epsilon_e$  were found between 0.0016 and 0.0026.

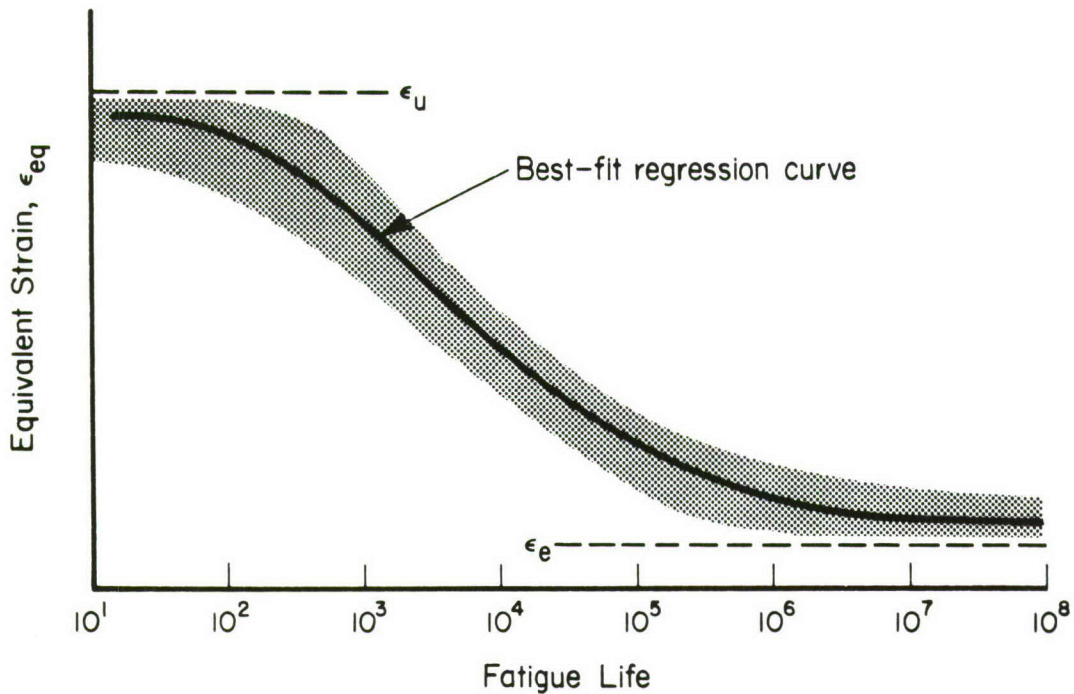


Figure 1. Schematic illustration of regressed inverse hyperbolic tangent curve and appropriate functional limits.

As a final step in the analysis, tolerance limits or probability of survival curves were established for each data set. The requirements and procedures involved in the development of these limits are included in Appendix A. Using a computer program, tolerance limits were evaluated at small increments within the range of data to form piecewise continuous probability of survival curves. Two curves were generated for each data set, and they were developed to represent 90 and 99 percent tolerance bands at a 95 percent confidence level.

Results of Fatigue Analysis – Table 1 summarizes the results of the analysis for selected data sets from each material. Graphical displays of the consolidated data are presented in Figures 2 through 9.

Notched and unnotched 2024-T3 and 7075-T6 sheet data are shown in Figures 2, 3, 4, and 5, respectively. For both aluminum alloys the consolidation was substantial, with the unnotched data displaying slightly better consolidation than the notched.

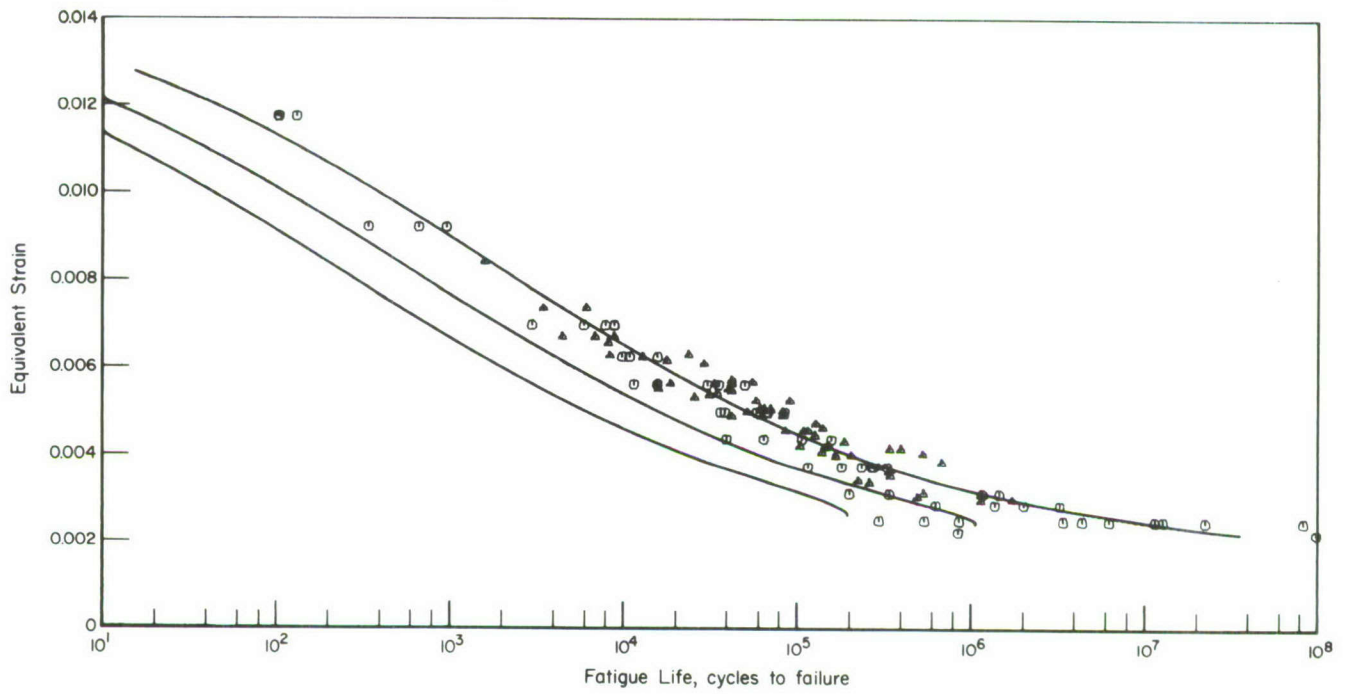


Figure 2. Consolidated 2024-T3 sheet data (unnotched) with fitted mean curve and 90 and 99 percent probability of survival lines.

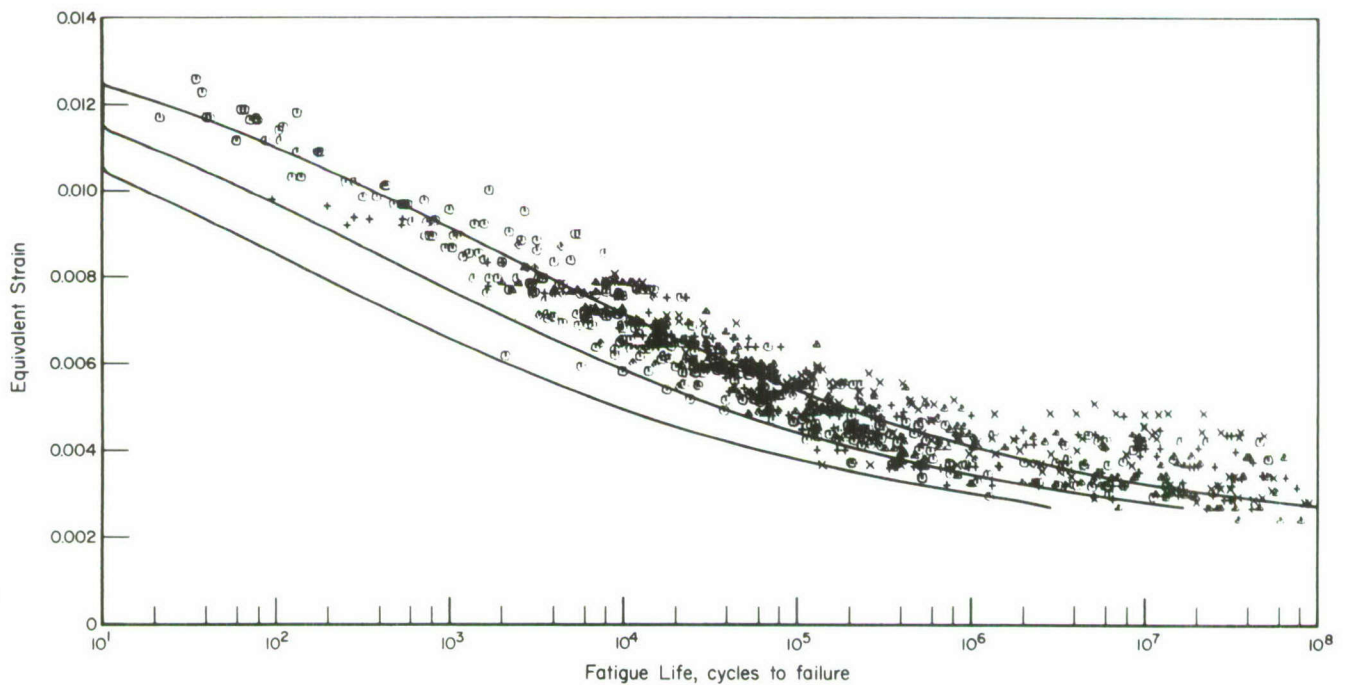


Figure 3. Consolidated 2024-T3 sheet data (notched) with fitted mean curve and 90 and 99 percent probability of survival lines.

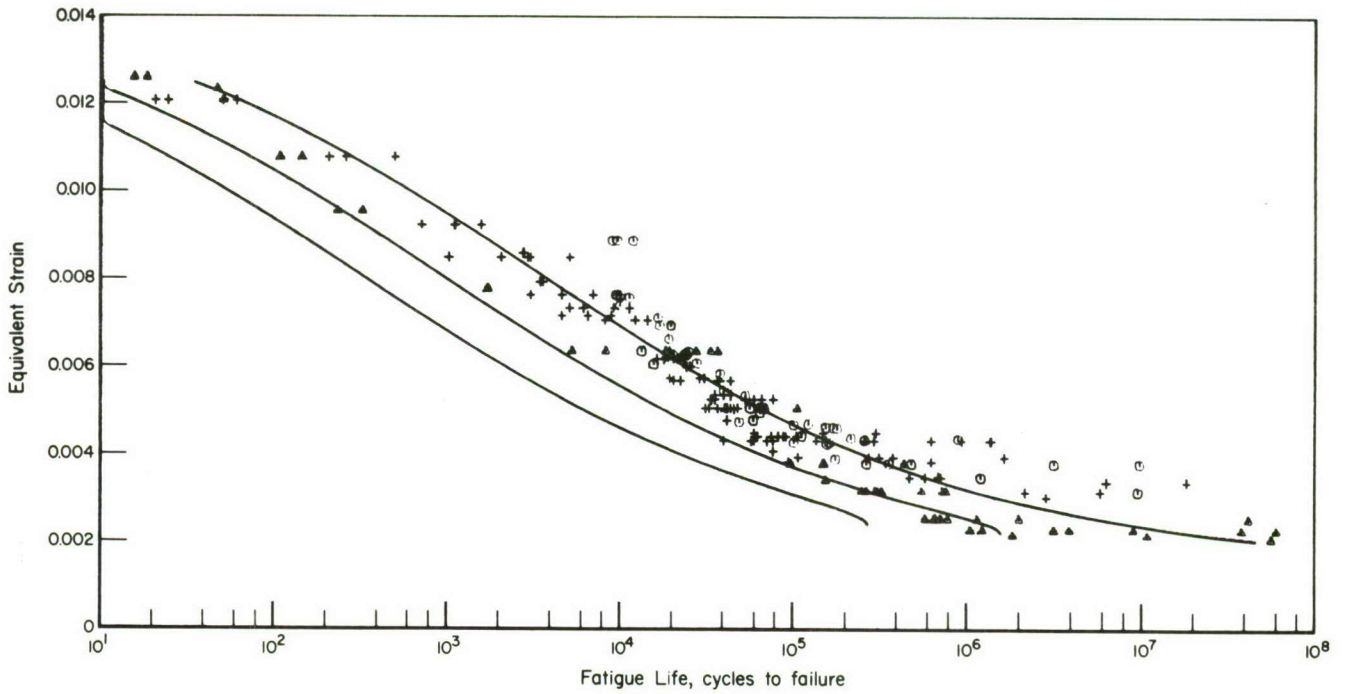


Figure 4. Consolidated 7075-T6 sheet data (unnotched) with fitted mean curve and 90 and 99 percent probability of survival lines.

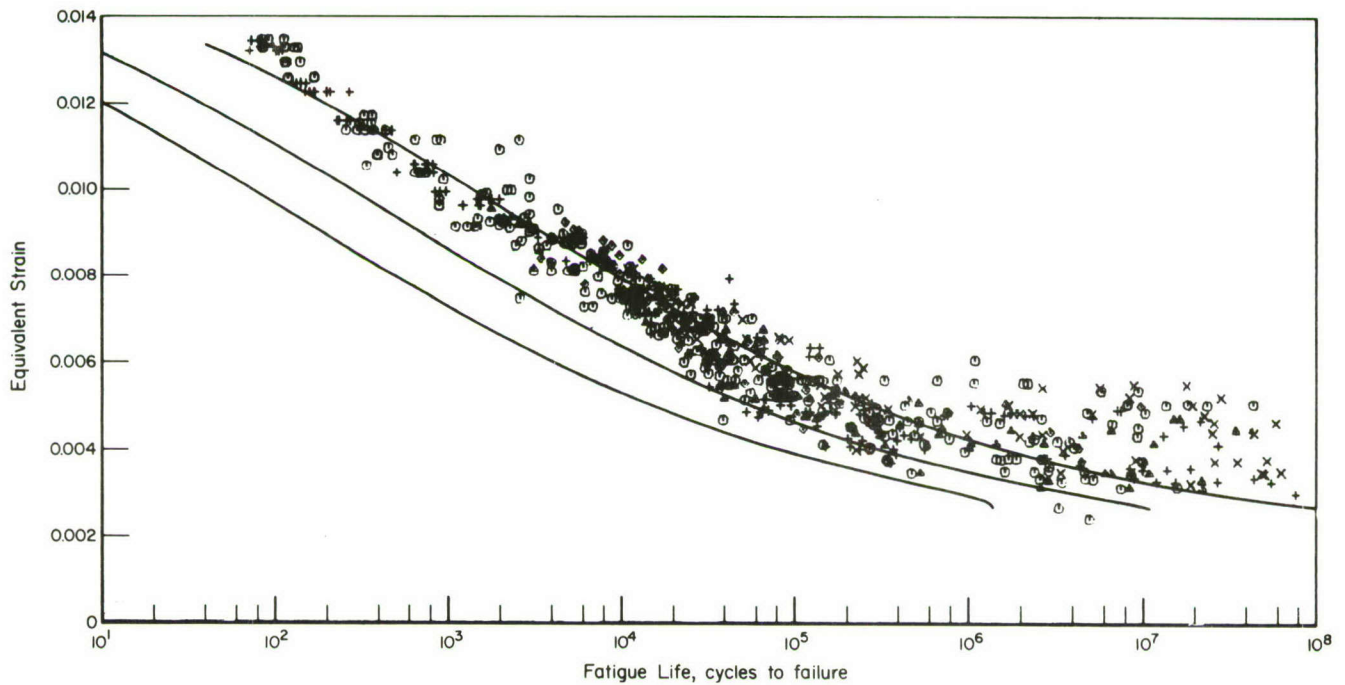


Figure 5. Consolidated 7075-T6 sheet data (notched) with fitted mean curve and 90 and 99 percent probability of survival lines.

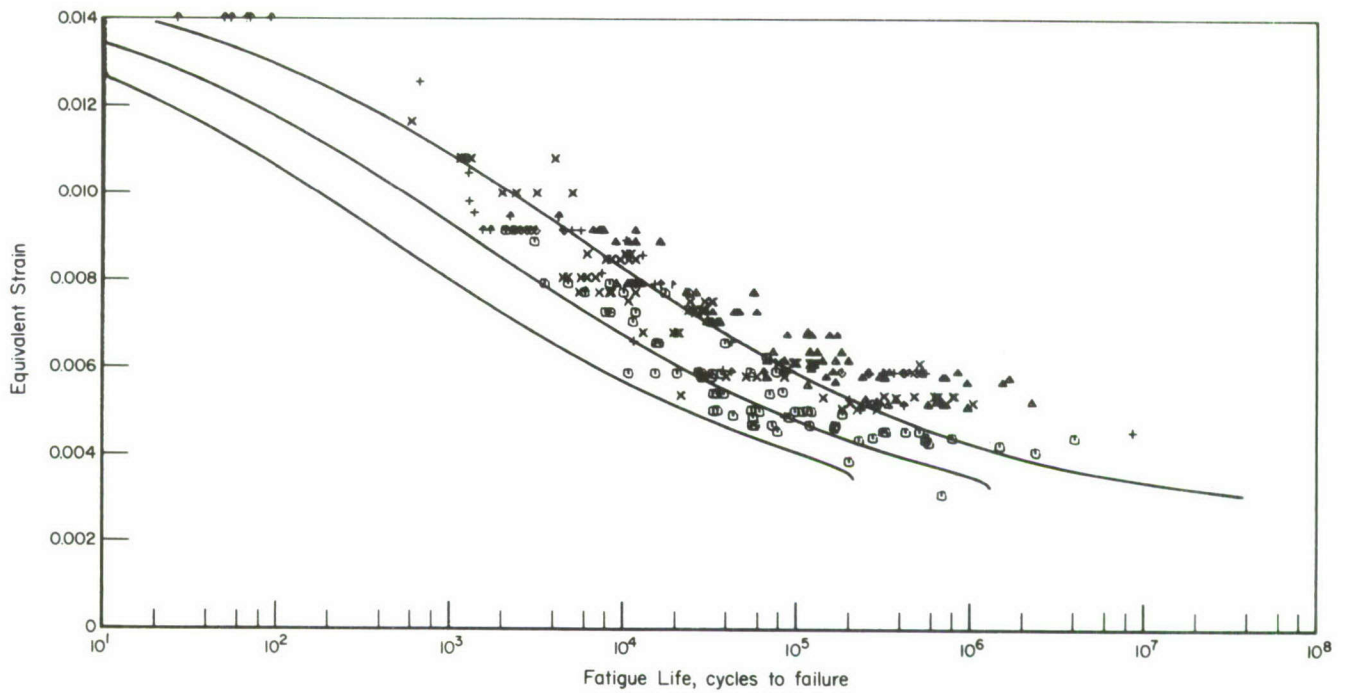


Figure 6. Consolidated 300M billet and forging data (unnotched) with fitted mean curve and 90 and 99 percent probability of survival lines.

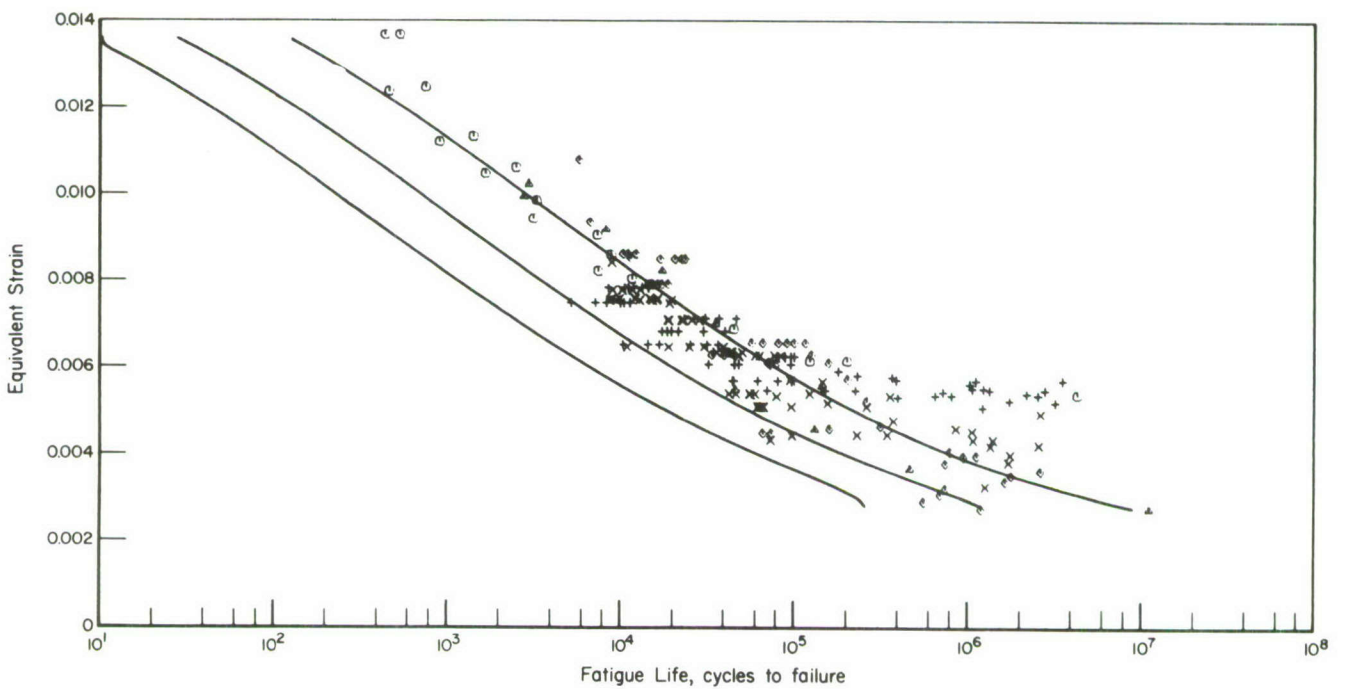


Figure 7. Consolidated 300M billet and forging data (notched) with fitted mean curve and 90 and 99 percent probability of survival lines.

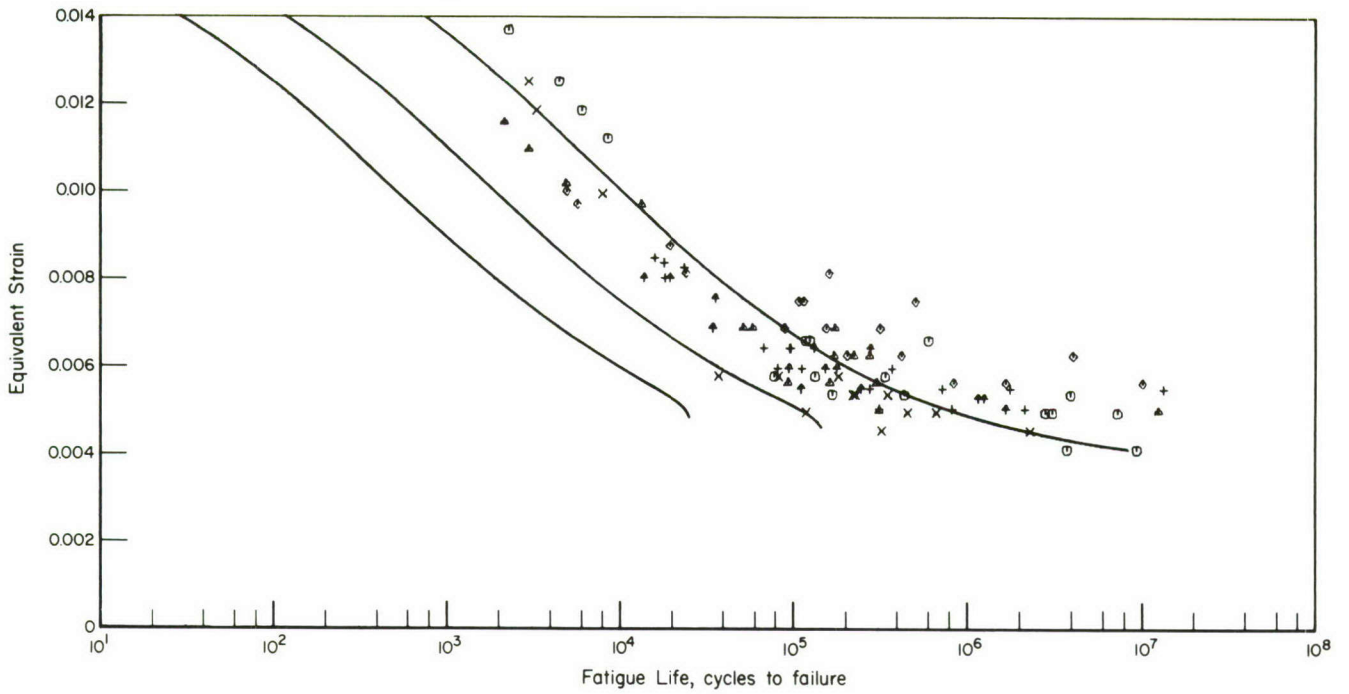


Figure 8. Consolidated STA Ti-6Al-4V sheet data (unnotched) with fitted mean curve and 90 and 99 percent probability of survival lines.

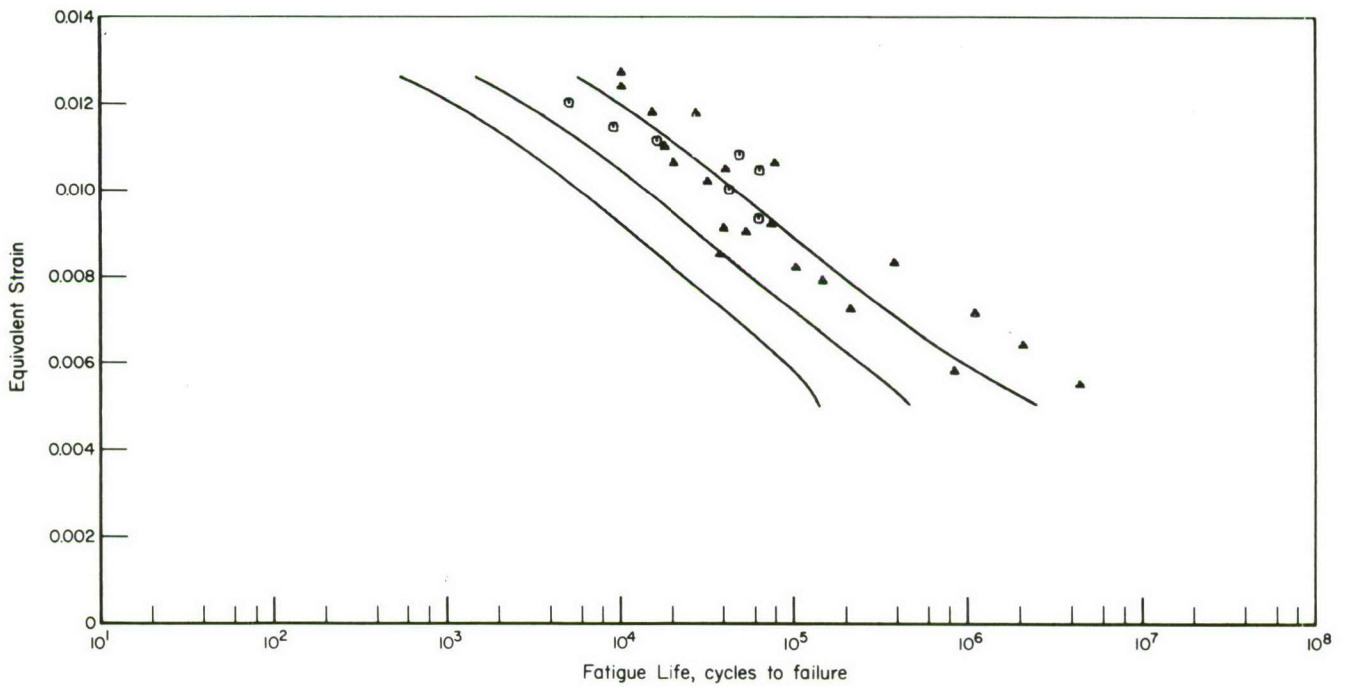


Figure 9. Consolidated STA Ti-6Al-4V sheet data (notched) with fitted mean curve and 90 and 99 percent probability of survival lines.

TABLE 1. RESULTS OF NOTCHED AND UNNOTCHED FATIGUE DATA CONSOLIDATION USING THE INVERSE HYPERBOLIC TANGENT FUNCTION WITH WEIGHTED EQUIVALENT STRAIN DATA

Material	Type of Data	Number of Data Points	Weighted $R^2$ , percent	Regression Coefficients		Limits Employed	
				$A_0$	$A_1$	$\epsilon_u$	$\epsilon_e$
2024-T3 Sheet	Unnotched <sup>(7,8)</sup>	121	98.9	4.644	2.914	0.0152	0.0018
	Notched <sup>(9-15)</sup>	887	96.8	4.867	3.417	0.0150	0.0021
7075-T6 Sheet	Unnotched <sup>(8,16)</sup>	220	97.3	4.899	2.809	0.0150	0.0016
	Notched <sup>(9-16)</sup>	695	96.3	4.969	3.313	0.0170	0.0020
300M Billet and Forging	Unnotched <sup>(17-21)</sup>	289	90.4	4.796	2.565	0.0154	0.0026
	Notched <sup>(17-21)</sup>	218	89.2	5.259	3.073	0.0161	0.0023
STA Ti-6Al-4V Sheet <sup>a</sup>	Unnotched <sup>(22)</sup>	98	95.1	4.565	1.967	0.0160	0.0020
	Notched <sup>(22)</sup>	96	85.0	6.905	3.909	0.0170	0.0020

<sup>a</sup> Monotonic and cyclic stress-strain calculations were based on data from Ti-6Al-4V bar.

- (7) Grover, H. J., Bishop, S. M., and Jackson, L. R., "Fatigue Strength of Aircraft Materials Axial-Load Fatigue Tests on Unnotched Sheet Specimens of 24S-T3 and 75S-T6 Aluminum Alloys and of SAE 4130 Steel", NACA TN 2324 (1951).
- (8) Illg, W., "Fatigue Tests on Notched and Unnotched Sheet Specimens of 2024-T3 and 7075-T6 Aluminum Alloys and of SAE 4130 Steel with Special Consideration of the Life Range from 2 to 10,000 Cycles", NACA TN 3866 (1959).
- (9) Grover, H. J., Bishop, S. M., and Jackson, L. R., "Fatigue Strengths of Aircraft Materials Axial-Load Fatigue Tests on Notched Sheet Specimens of 24S-T3 and 75S-T6 Aluminum Alloys and of SAE 4130 Steel with Stress-Concentration Factors of 2.0 and 4.0", NACA TN 2389 (1951).
- (10) Grover, H. J., Bishop, S. M., and Jackson, L. R., "Fatigue Strengths of Aircraft Materials Axial-Load Fatigue Tests on Notched Sheet Specimens of 24S-T3 and 75S-T6 Aluminum Alloys and of SAE 4130 Steel with Stress-Concentration Factor of 5.0", NACA TN 2390 (1951).
- (11) Grover, H. J., Hyler, W. S., and Jackson, L. R., "Fatigue Strengths of Aircraft Materials Axial-Load Fatigue Tests on Notched Sheet Specimens of 24S-T3 and 75S-T6 Aluminum Alloys and SAE 4130 Steel with Stress-Concentration Factor of 1.5", NACA TN 2639 (1952).
- (12) Hardrath, H. F., and Illg, W., "Fatigue Tests at Stresses Producing Failure in 2 to 10,000 Cycles, 24S-T3 and 75S-T6 Aluminum Alloy Sheet Specimens with a Theoretical Stress-Concentration Factor of 4.0 Subjected to Completely Reversed Axial Load", NACA TN 3132 (1954).

Results for the 300M steel fatigue analysis are presented in Figures 6 and 7. The  $R^2$  values for both curves were not as high as the values determined for the aluminum alloys, but the overall data collapse was considered good since the inherent data scatter for this material was much larger than for the aluminum alloys.

Plots of consolidated Ti-6Al-4V sheet data are shown in Figures 8 and 9. All titanium data were found to be very difficult to analyze due to large inherent data scatter and to insufficient information concerning cyclic stress-strain behavior of various titanium product forms and heat treatments. Despite these factors, a reasonably good data consolidation was accomplished.

### Summary and Conclusions

As a result of this study, it was found that large amounts of constant-amplitude fatigue data generated at different stress ratios and notch

- (13) Landers, C. B., and Hardrath, H. F., "Results of Axial-Load Fatigue Tests on Electropolished 2024-T3 and 7075-T6 Aluminum Alloy Sheet Specimens with Central Holes", NACA TN 3631 (1956).
- (14) Grover, H. J., Hyler, W. S., and Jackson, L. R., "Fatigue Strengths of Aircraft Materials Axial-Load Fatigue Tests in Edge-Notched Sheet Specimens of 2024-T3 and 7075-T6 Aluminum Alloys and of SAE 4130 Steel with Notch Radii of 0.004 and 0.070 Inch", NASA TN D-111 (1959).
- (15) Naumann, E. C., Hardrath, H. F., and Guthrie, D. E., "Axial-Load Fatigue Tests of 2024-T3 and 7075-T6 Aluminum-Alloy Sheet Specimens Under Constant- and Variable-Amplitude Loads", NASA TN D-212 (1959).
- (16) Smith, C. R., "S-N Characteristics of Notched Specimens", NASA CR-54503 (1966).
- (17) Bateh, E. J., and McGee, W., "Axial Load Fatigue and Tensile Properties of 300 VAR Steel Heat Treated to 280-300 ksi", ER-10202 (MCIC 74342), Lockheed-Georgia Company (1969).
- (18) Harmsworth, C. L., "Low-Cycle Fatigue Evaluation of Titanium 6Al-6V-2Sn and 300M Steel for Landing Gear Applications", AFML-TR-69-48 (1969).
- (19) Deel, O. L., and Mindlin, H., "Engineering Data on New and Emerging Structural Materials", AFML-TR-70-252 (1970).
- (20) Jaske, C. E., "The Influence of Chemical Milling on Fatigue Behavior of 300M VAR Steel", Final Report (April, 1969).
- (21) Jaske, C. E., "The Influence of Variation in Decarburization Level Upon Fatigue Life of 300M VAR Steel", Letter Report to the Bendix Corporation (September 30, 1968).
- (22) Anon., "Determination of Design Data for Heat Treated Titanium Alloy Sheet", Vol. 3 - Tables of Data Collected, ASD-TDR-335, Lockheed-Georgia Company (1962).

concentrations can be consolidated for use in design applications. The developed consolidation methods were tested on large quantities of data gathered on 2024 and 7075 aluminum alloys, Ti-6Al-4V alloy, and 300M steel.

Specific conclusions drawn in the course of this program are

- (1) The Walker equivalent strain parameter can be used to account for effects of stress ratio.
- (2) A local stress-strain analysis, which uses a computed  $K_f$  value and a technique to approximately account for relaxation of mean stress, can be used to account for notch effects.
- (3) An inverse hyperbolic tangent function can be employed to model fatigue curves in terms of  $\epsilon_{eq}$  versus  $\log N_f$  for both unnotched and notched specimens.
- (4) Using the  $\tanh^{-1}$  function, it is possible to compute mean fatigue curves and tolerance limit curves for each combined data set. In this work, 90 and 99 percent probability of survival limits were developed at a 95 percent confidence level.
- (5) Weighting factors can be used to increase uniformity in fatigue data variances.

#### FATIGUE-CRACK PROPAGATION

As an outgrowth of the increasing interest in damage-tolerant design concepts, the characterization of fatigue-crack propagation is a vital link between the crack initiating phenomenon of fatigue and the critical instability of cracked structural elements as identified by fracture toughness and residual strength. In small-size, laboratory fatigue specimens, crack initiation and specimen failure may be nearly synonymous. However, in larger structural components, the existence of a crack does not necessarily imply imminent failure of the component. Substantial and useful structural life is accountable in the cyclic crack extension (subcritical crack growth) which can be tolerated prior to reaching conditions critical for fracture.

As a natural extension of the inclusion of fatigue, fracture toughness and residual strength information in MIL-HDBK-5B, fatigue-crack-propagation information is being considered for incorporation into this

document. The phenomenon of fatigue-crack propagation, its characterization and the means of incorporating such material behavior data in MIL-HDBK-5B are considered in the following discussion.

### Fatigue-Crack-Propagation Behavior

As a physical or mechanical phenomenon, fatigue-crack propagation may be described as the growth or extension of a crack in a structural member under cyclic loading. Experimental data of this type are generally defined as crack-growth data and are displayed in a crack-growth curve as illustrated in the left-hand portion of Figure 10.

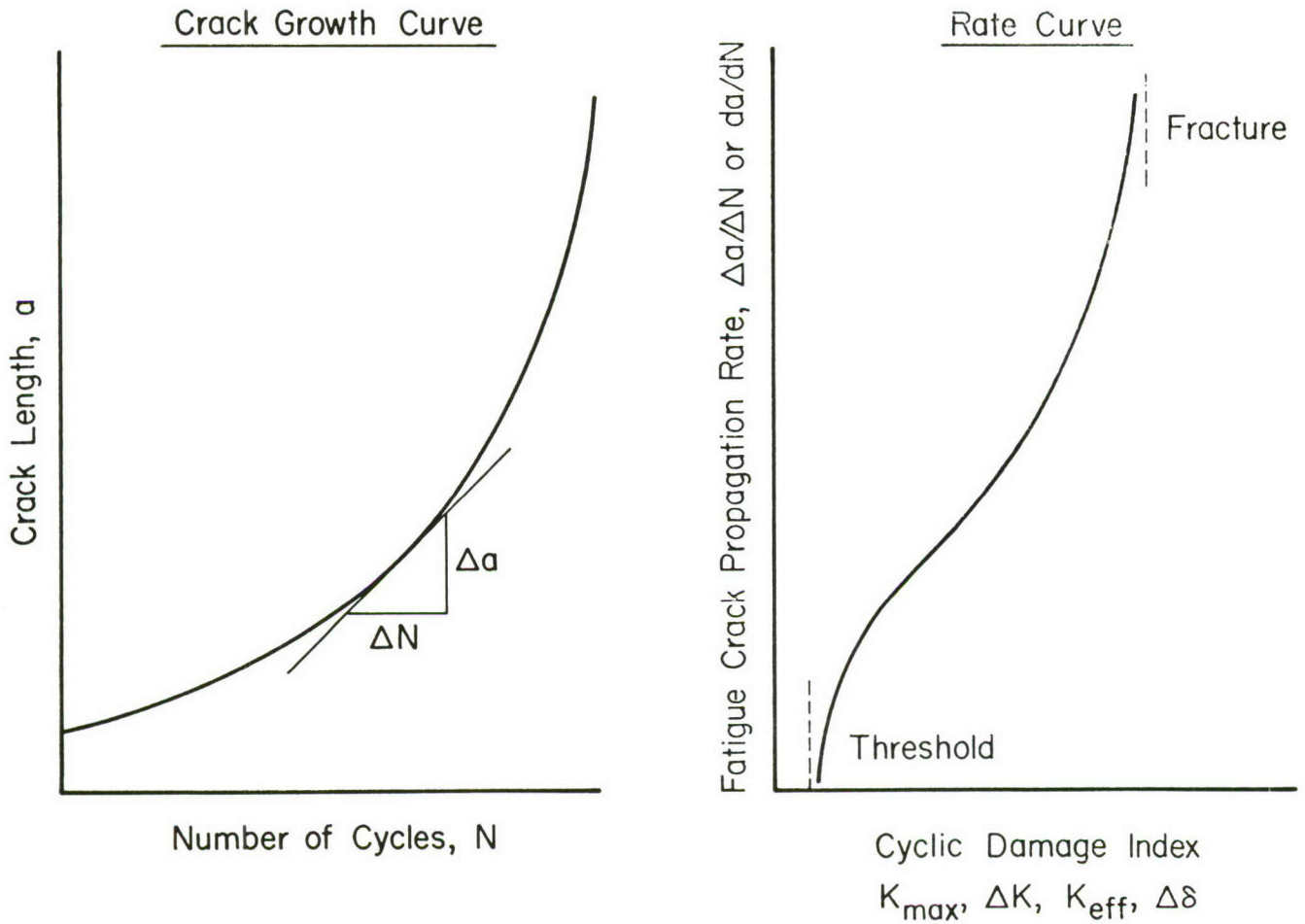


Figure 10. Presentation of fatigue-crack-growth data.

Since the crack-growth curve is dependent on the initial crack length and the loading condition, the presentation of crack-growth curves is not the most concise means of representing crack behavior in a material. As with most dynamic processes, the rate behavior or slope,  $\Delta a/\Delta N$ , of the crack-growth curve provides a more fundamental characterization of the behavior. In general, the fatigue-crack-propagation rate behavior can be evaluated as a function of a cyclic damage index, as illustrated in the right-hand portion of Figure 10. A number of useful expressions for the cyclic damage index have been achieved with the stress intensity factor concepts of linear elastic fracture mechanics.

The task of formulating a method for the analysis of fatigue-crack-propagation data consists primarily of determining a suitable functional relationship between  $\Delta a/\Delta N$  and a cyclic damage index. Such a functional relationship is referred to as a fatigue-crack-propagation model. Based on the general observations of rate behavior, a useful model must satisfy the following requirements:

- (1) It must accommodate threshold effects of rapidly decaying crack-growth rates at low levels of applied stress-intensity factor.
- (2) It must accommodate the terminal effect of rapidly accelerating crack-growth rates as crack extension approaches a critical fracture condition.
- (3) It must have a quasi-linear behavior in the central range transitory to the above threshold and terminal conditions.
- (4) It should compress the layering due to stress ratio effects.
- (5) It should be usable as an integration tool to perform the inverse operation of accumulating incremental damage and reconstructing the crack-growth curve.

An approach to the formulation of the crack cyclic damage index and the functional relation are described in the next section.

#### Fatigue-Crack-Propagation Analysis Independent Variation Formulation -

It is known that fatigue-crack-propagation behavior is influenced by maximum cyclic stress,  $S_{\max}$ , and some measure of the cyclic stress range,  $\Delta S$  (such as

stress ratio, R, or minimum cyclic stress,  $S_{\min}$ ), the instantaneous crack size, a, and other factors such as frequency, temperature, and environment. Thus, fatigue-crack-propagation rate behavior can be characterized, in general form, by the relation

$$\Delta a/\Delta N = g(S_{\max}, \Delta S \text{ or } R \text{ or } S_{\min}, a, \dots) \quad (10)$$

By applying the concepts of linear elastic fracture mechanics, the stress and crack size parameters can be combined into the stress intensity factor parameter, K, such that Equation (10) may be simplified to

$$\Delta a/\Delta N = g(K_{\max}, \Delta K, \dots) \quad (11)$$

where  $K_{\max}$  is the maximum cyclic stress intensity factor, and  $\Delta K$  is the range of the cyclic stress intensity factor.

Although the relative influences of  $K_{\max}$  and  $\Delta K$  are not known precisely, these variables can be coupled through an exponential parameter, m, varying from zero to unity such that an apportionment of  $K_{\max}$  and  $\Delta K$  influences can be evaluated. By using the relation,

$$\Delta K = (1-R) K_{\max} \quad (12)$$

a simplification of Equation (11) may be expressed as

$$\Delta a/\Delta N = g \left[ (1-R)^m K_{\max} \right] \quad (13)$$

The condition that m equals zero implies that the maximum cyclic stress intensity factor alone is significant. The condition that m equals unity implies that only the cyclic stress intensity factor range is significant. In reality, it appears that m is some intermediate value which defines the true interrelationship of these parameters. The determination of this intermediate value, if it exists, has been an objective of a current Battelle research program.

In analyzing fatigue-crack-propagation rate behavior, it is apparent that a sigmoidally shaped curve is required to model the data on a doubly logarithmic graphical format. The choice for the relation between  $\Delta a/\Delta N$  and K of the inverse hyperbolic-tangent function suggested by Collipriest<sup>(23)</sup>

---

(23) Collipriest, J. E., "An Experimentalist's View of the Surface Flaw Problem", The Surface Crack: Physical Problems and Computational Solutions, ASME, New York (1972), pp 43-62.

satisfied this criterion. The essence of his model has been generalized in terms of an effective stress-intensity factor,  $K_{\text{eff}}$ , expressed as

$$K_{\text{eff}} = K_{\text{max}} (1-R)^m = K_{\text{max}}^{(1-m)} (\Delta K)^m \quad (14)$$

The formulation of the analytical model which was developed for representing fatigue-crack-propagation rate behavior is

$$\log \frac{da}{dN} = C_1 + C_2 \tanh^{-1} \left[ \frac{\log [K_c K_o / (K_{\text{max}} (1-R)^m)^2]}{\log (K_o / K_c)} \right], \quad (15)$$

where  $K_c$  = plane stress critical fracture toughness  
 $K_o$  = crack propagation threshold stress intensity factor  
 $K_{\text{max}}$  = maximum cyclic stress intensity factor  
 $R$  = stress ratio  
 $m$  = coupling exponent  
 $C_1, C_2$  = regression derived coefficients.

The coupling exponent,  $m$ , reflects the interaction of  $K_{\text{max}}$  and  $\Delta K$ . The coefficient  $C_1$  defines the midrange rate; the coefficient  $C_2$  defines the minimum slope value of the modeling curve.

The results of this analysis for several aerospace structural materials are summarized in Table 2. Graphical displays are presented in Figures 11 through 15 for the respective materials. The best-fit regression curve is represented by the central solid line through the data points. On either side of the average-curve are the 90 and 99 percent tolerance limits, with a 95 percent level of confidence.

### Conclusions

A concise consolidation of fatigue-crack-propagation rate data can be achieved with Equation (15) which can accommodate a wide range of  $R$  values (presently demonstrated  $-1.0 > R > 0.8$ ). This procedure appears to be well suited to handbook presentation. However, to realize maximum utilization, additional effort is required to perform the design task or inverse operation (i.e., crack damage accumulation) for life prediction, and to define a method for selecting  $K_o$  and  $K_c$ .

Preliminary guidelines delineating this newly developed analytical technique and the method of presenting fatigue-crack-propagation data in

TABLE 2. RESULTS OF REGRESSION ANALYSIS AND COEFFICIENTS FOR SIGMOIDAL MODEL

Material	n, Number of Data Points	$C_1$	$C_2$	m	$K_{O_3}/2$ MN/m <sup>3/2</sup> (ksi-in. <sup>1/2</sup> )	$K_{C_3}/2$ MN/m <sup>3/2</sup> (ksi-in. <sup>1/2</sup> )	R <sup>2</sup>	SSD	$\sigma$	$\bar{X}$	$\Sigma(X-\bar{X})^2$
2024-T3	3,378	-4.489	3.487	0.420	2.20 (2.00)	142.74 (130.00)	0.906	273.00	0.284	0.106	179.85
7075-T6	746	-4.207	2.241	0.320	3.29 (3.00)	85.64 (78.00)	0.912	47.28	0.252	0.178	79.34
7075-T7351	1,082	-4.042	2.574	0.350	4.36 (4.00)	109.90 (100.00)	0.952	33.81	0.177	0.221	79.38
300M	513	-5.186	1.296	0.335	8.78 (8.00)	65.88 (60.00)	0.661	28.56	0.236	0.00024	27.21
Ti-6Al-4V	782	-4.046	2.825	0.580	4.39 (4.00)	274.50 (250.00)	0.982	36.14	0.215	-0.161	161.20

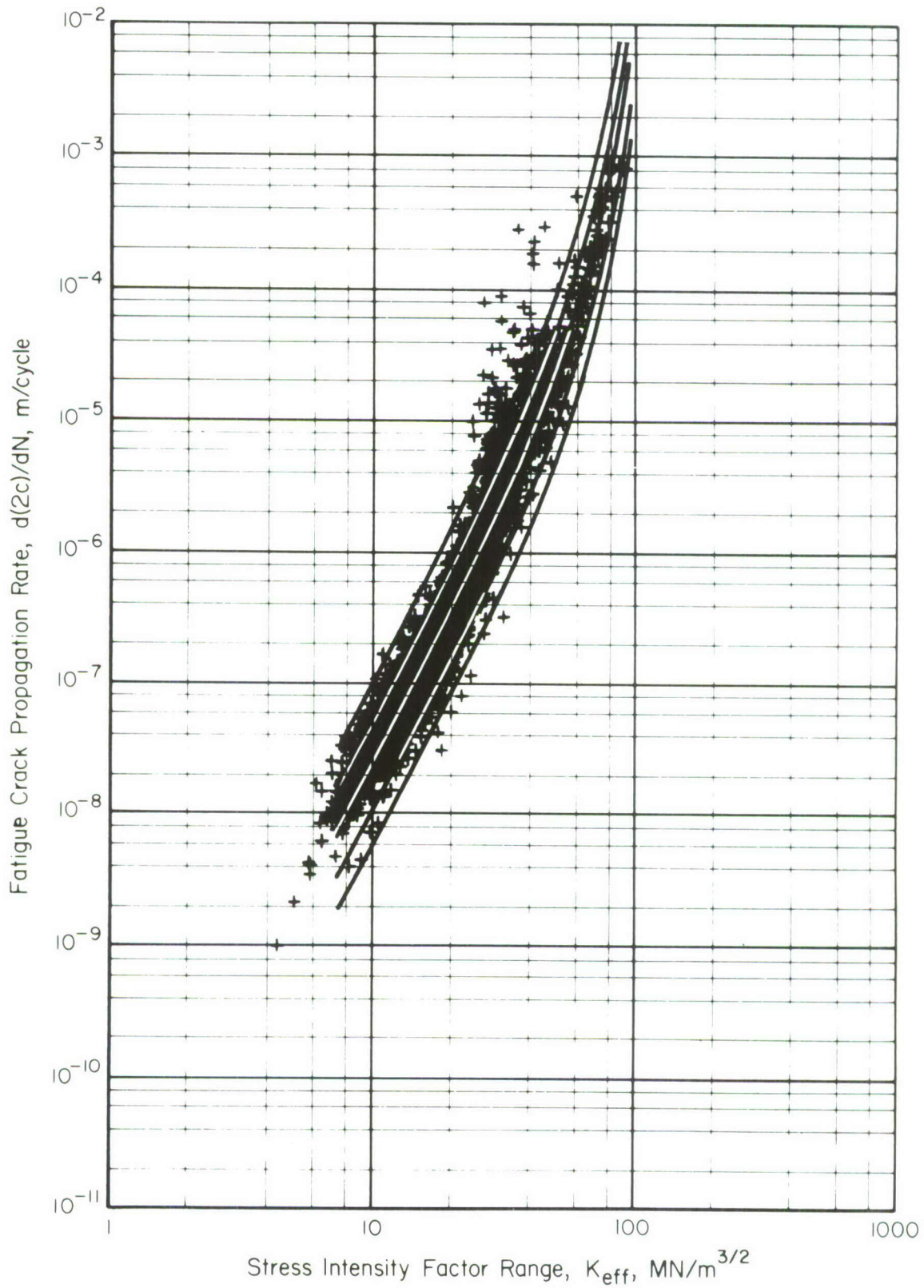


Figure 11. Fatigue-crack-propagation-rate curve for 2024-T3 aluminum alloy.

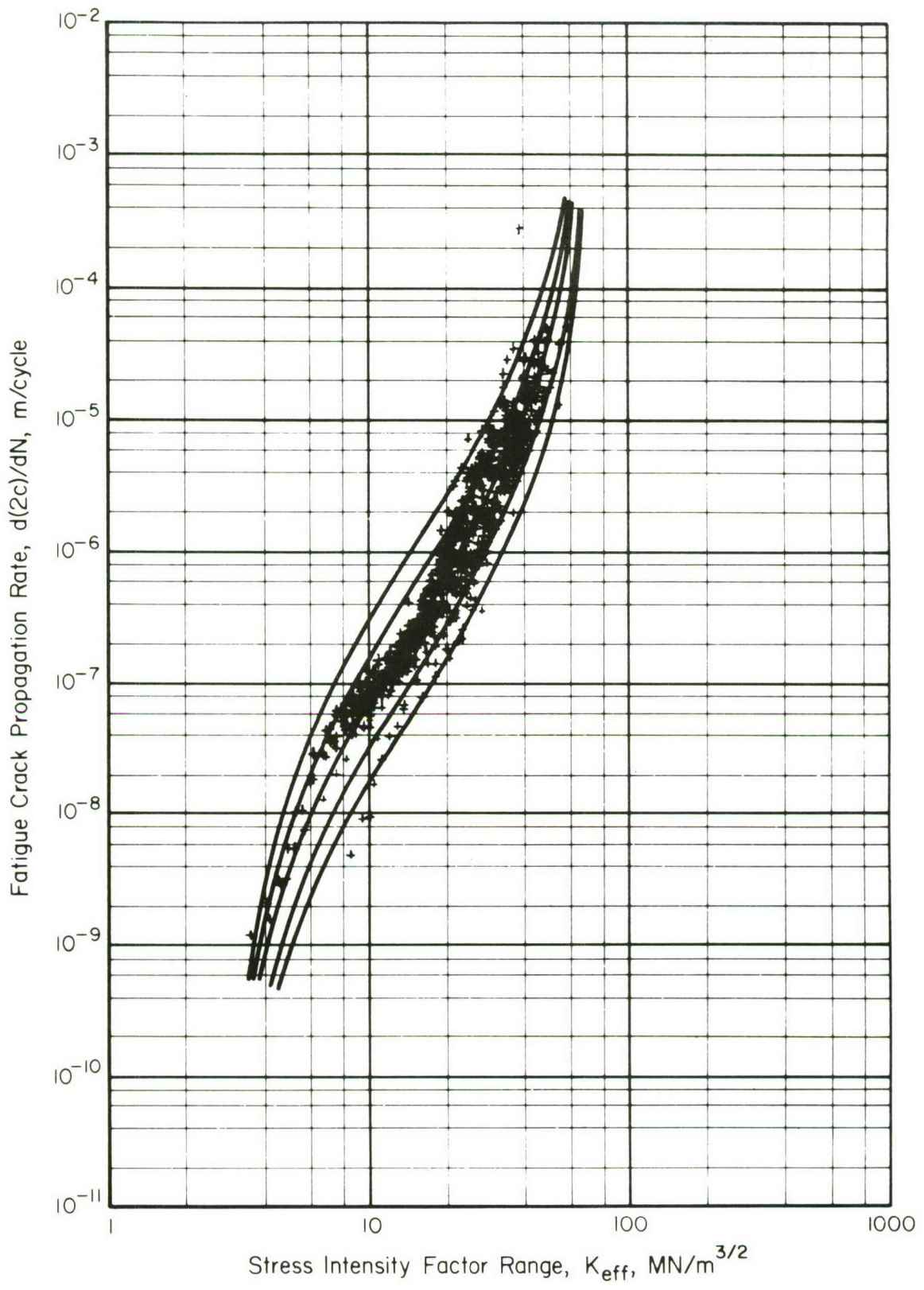


Figure 12. Fatigue-crack-propagation-rate curve for 7075-T6 aluminum alloy.

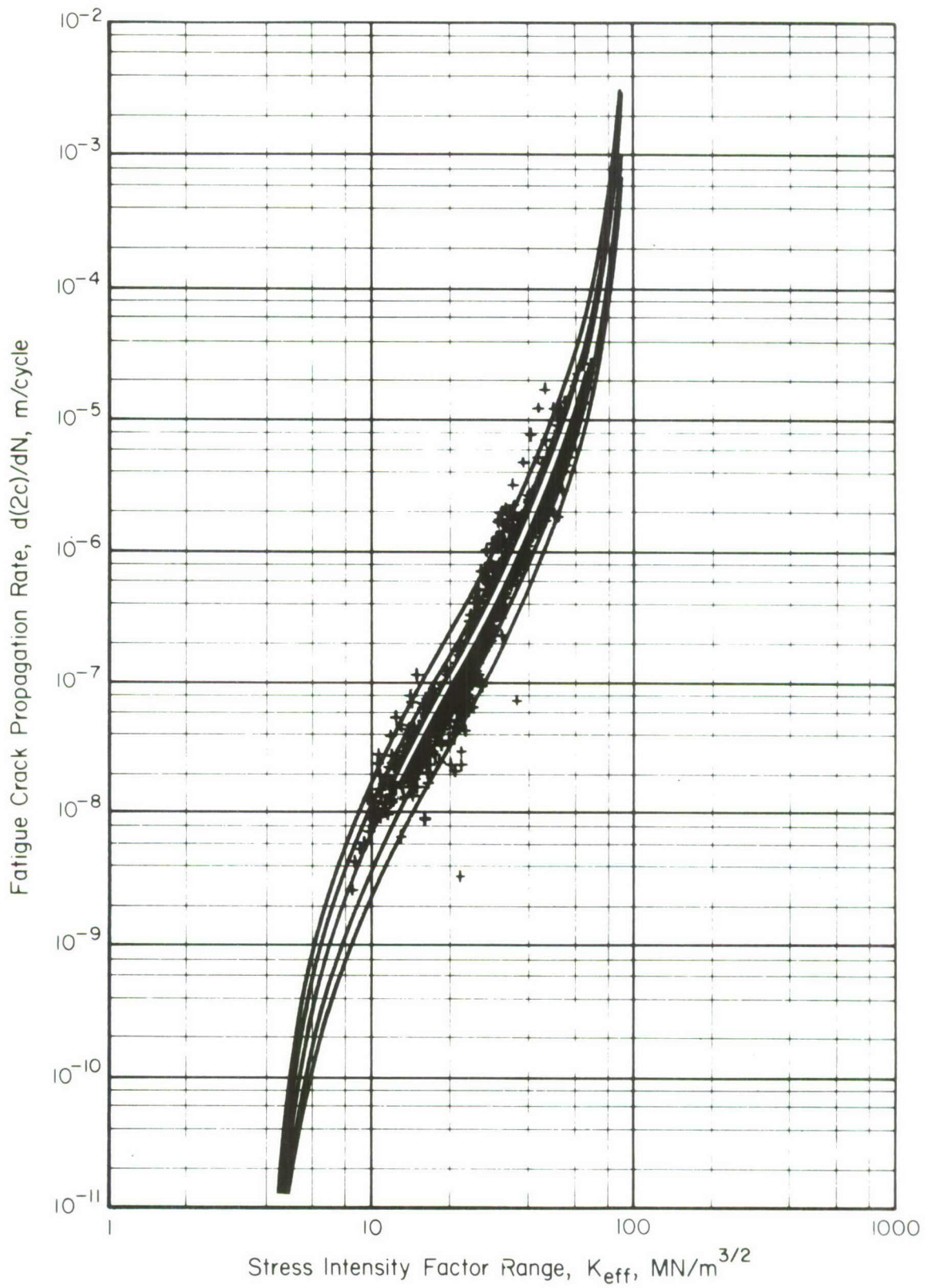


Figure 13. Fatigue-crack-propagation-rate curve for 7075-T7351 aluminum alloy.

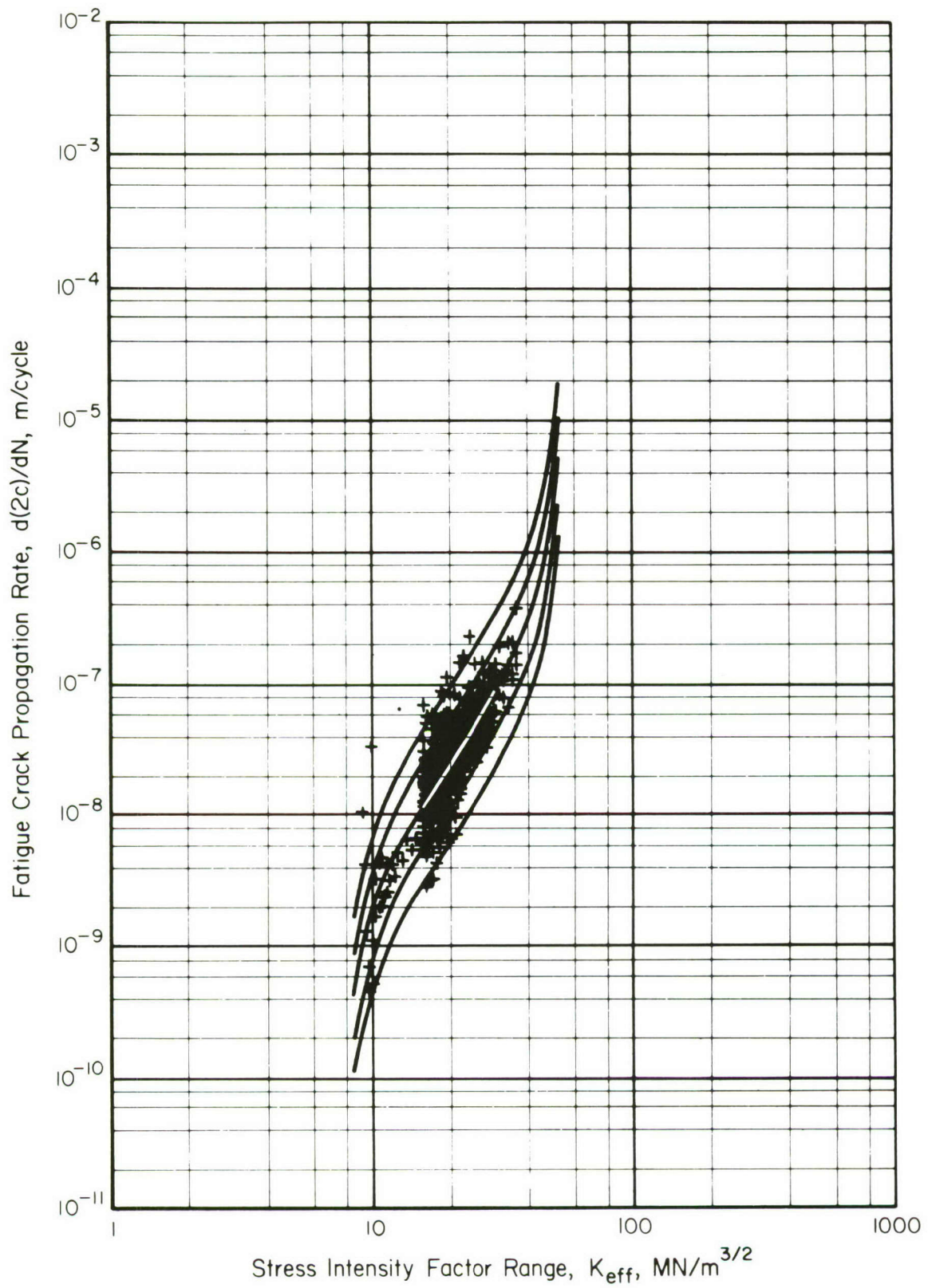


Figure 14. Fatigue-crack-propagation curve for 300M steel.

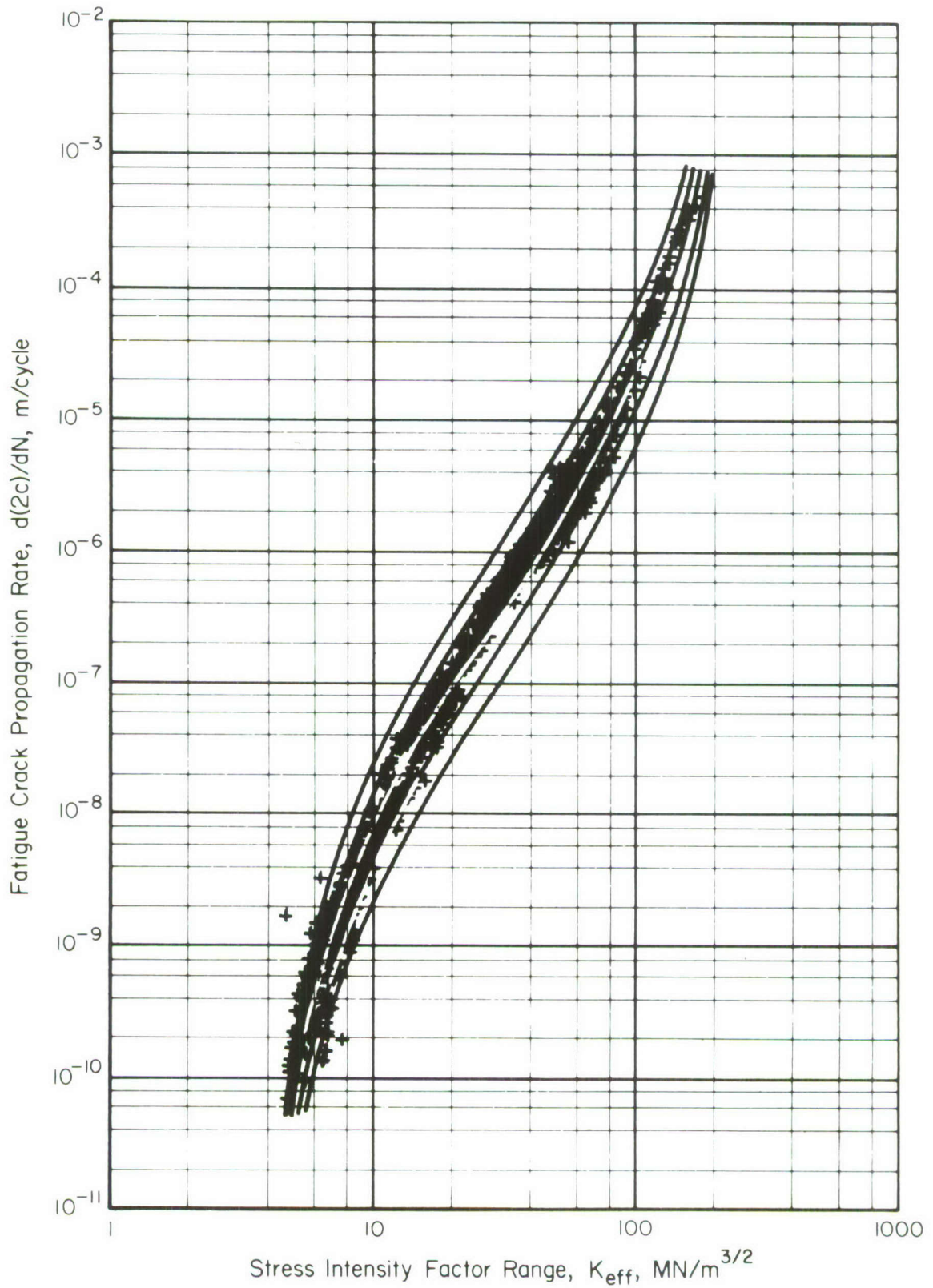


Figure 15. Fatigue-crack-propagation-rate curve for Ti-6Al-4V alloy.

MIL-HDBK-5B are being prepared and will be presented to the MIL-HDBK-5 Coordination Activity for discussion at the April 23-25, 1974 meeting.

## FRACTURE TOUGHNESS

Unexpected fractures and failures of structural components due to the initiation and propagation of cracks have been of increasing concern to the aerospace community during the past fifteen years. Although cracks are obviously undesirable, they are generally an unavoidable circumstance in the processing, fabrication, and service of a structural material. Cracks may form and grow from minor flaws and defects in a material or from design discontinuities such as access or fastener holes, and transition fillets. All such flaws and discontinuities may act as localized stress-raisers and may be the source of cracks which lead to structural failure at loads below those of the nominal design.

For a material to be of value in structural applications, it must have some resistance to fracture in the presence of defects. This resistance to fracture in the presence of cracks, design discontinuities and other flaws is termed fracture toughness. Many measures of fracture toughness have evolved. Those based on fundamental qualities of stress, flaw size, and structural configuration have been proven to be most amenable to use in design applications. Other measures based on energy considerations are very useful for qualitative evaluation of materials, but they have proved to be difficult to apply to specific design configurations.

The current philosophy which has been adopted in MIL-HDBK-5B to characterize fracture behavior is presented in this portion of the report.

### Fracture Parameters

With the advent of linear elastic fracture mechanics, the stress-intensity factor concept has dominated most quantitative engineering studies of fracture behavior. The stress-intensity factor is a quantity describing the intensity of the stress-strain field at the tip of a crack in a loaded structural element. The gross stress and the crack size are characterized parametrically by the stress-intensity factor,  $K$ , in the relation

$$K = f\sqrt{\pi a} Y \quad , \quad (16)$$

where  $f$  = stress applied to the gross section

$a$  = crack size

$Y$  = nondimensional geometric factor scaling crack size with structural size.

Roman numeral subscripts, I, II, and III on  $K$  are utilized to denote, respectively, the opening, sliding, and tearing modes of crack surface displacement. Mode I has been evaluated almost exclusively in current data generation programs.

### Fracture Behavior

The fracture mechanism is a complex process which has many interpretations dependent on the technical disciplines involved. For the structural designer, a convenient illustration of the fracture mechanism is the load-compliance record typical of a structural component containing a flaw. Such a record is shown in Figure 16.

In the most general case, flaw propagation proceeds in two stages-- a stable, slow growth followed by an unstable, rapid growth. (The slow growth phase includes all transitional behavior which does not result in rapid fracture. As such, it includes the short, quick bursts of crack growth as well as continuous processes of slow crack growth illustrated in Figure 16.) During initial loading of the structural component, the elastic load-compliance record is linear. Then, as the localized stress at the flaw tip reaches a threshold value, frequently denoted as "pop-in", the flaw begins to enlarge. This is the first notable deterioration of the structure and is an irreversible process. At this point the component may have considerable residual load-bearing capability which will allow the flaw to propagate in a slow and stable fashion under a steady or an increasing load. During the slow growth phase, in addition to the advancement of the crack front, there is an increase in plastic effects forward of the crack. As the flaw increases in size, the residual strength becomes less. When the residual strength vanishes, the flaw is at a critical size for rapid propagation and the component sustains its maximum load. The flaw then propagates suddenly and completely through the cross section, and the component fractures.

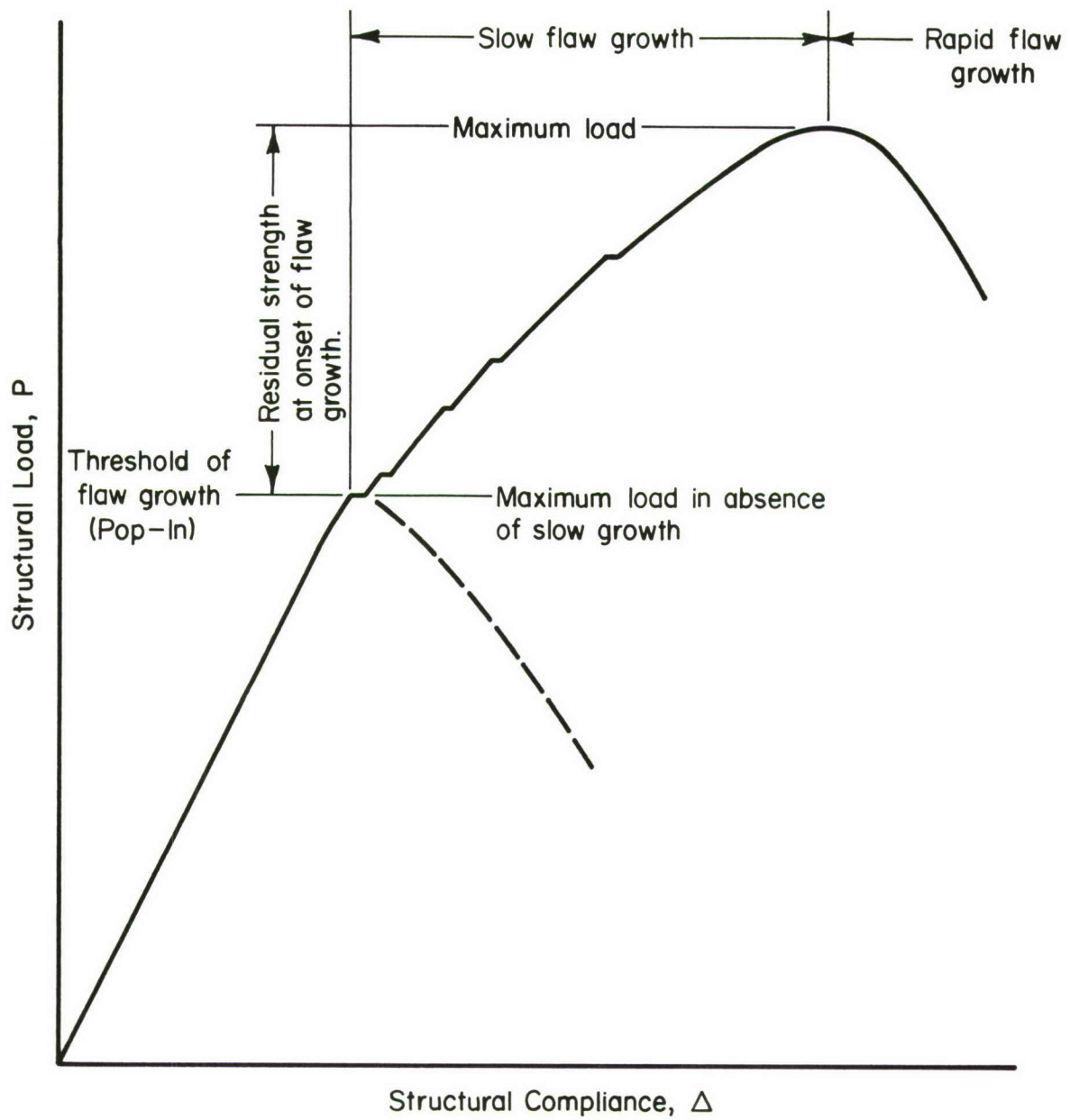


Figure 16. Typical load-compliance record of a structural component containing a flaw.

In addition to the two extremes discussed above, there may exist a myriad of transitional cases. Depending on the interaction of material ductility and the third dimensional restraint of thickness or bulk, intermediate degrees of slow growth can occur. This is frequently termed the "size or thickness effect" and reflects the degree of transition between a biaxial and triaxial stress state at the flaw front.

### Significance of Stress State

A primary factor in the fracture behavior of a material is the stress state, i.e., plane stress or plane strain. These stress states may be interpreted mechanically as a size or thickness effect within the material. The ideal plane-stress condition occurs in the two-dimensional case ( $t = 0$ ), in which all stresses are restricted to one plane. The material can accommodate extensive plastic deformation adjacent to the flaw prior to fracture and at fracture exhibit a relatively high  $K$  value. At the opposite extreme is the ideal plane-strain case in which the third dimension is of infinite extent so that the bulk restraint of the material permits no out-of-plane strains. As a result, plastic deformation is restricted, and the material fractures in a nearly elastic manner at a relatively low  $K$  value. In real materials, these ideal extremes can be closely approximated by "quasi" conditions of "thin" and "thick" bodies. The variation in stress intensity at fracture over these extremes, and the transition stage between may be represented as in Figure 17.

### Fracture Data Presentation

Although the characterization and application of fracture toughness in design are still undergoing considerable development, it is sufficiently important as a design criteria that it has been considered desirable to include such information in MIL-HDBK-5B. To date, two areas of linear elastic fracture mechanics have been incorporated in MIL-HDBK-5B. These are plane-strain-fracture toughness,  $K_{Ic}$ , and the residual strength parameter,  $K_{app}$ . A synopsis of each approach is presented in the remaining sections. It should be remembered that this is a highly active research area and is subject to rapid change as new concepts evolve.

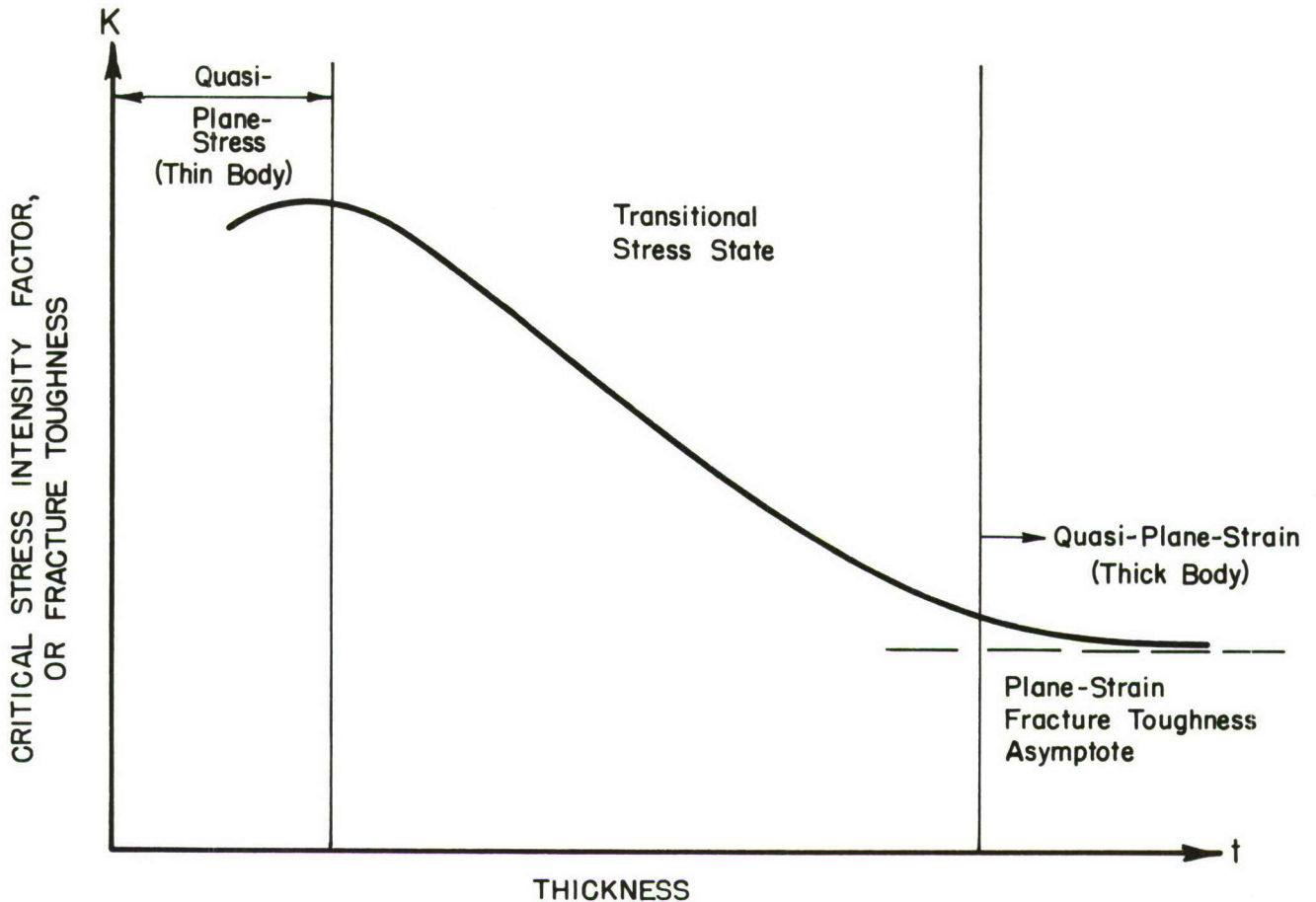


Figure 17. Variation of fracture toughness with thickness or stress state (size effect).

Plane-Strain Fracture Toughness – For materials which are inherently brittle or for structure and crack configurations which are in triaxial tension due to their thickness or bulk restraint, quasi-plane strain/stress conditions can be obtained in a finite-sized structural element. The triaxial stress state implicit to plane strain effectively embrittles the material by providing the maximum restraint against plastic deformation. In this condition, component behavior is essentially elastic until the fracture stress is reached (illustrated by the abrupt dashed line in Figure 16) and is readily amenable to analysis in terms of elastic fracture mechanics. This mode of fracture is frequently characteristic of the very high strength metals.

Two types of specimens have been evolved and are specified in ASTM Test Method E-399 for developing  $K_{Ic}$  information. These are the notch-bend

specimen and the compact-tension specimen, both of which offer material economics in testing. The critical dimensions, the analytical relations for determining  $K_{Ic}$ , and the recommended test procedures are provided in the test method. All  $K_{Ic}$  data in MIL-HDBK-5B have been obtained using these specimens and test method.

The objective of plane-strain fracture-toughness testing is to determine the stress and flaw size relationship under conditions of elastic fracture. The geometric constraints have been developed to obtain elastic fracture. However, experience indicates that for some materials there is frequently nonlinear behavior prior to fracture. Thus, ASTM Test Method E-399 contains the details involved in the analysis of fracture data that assure that the fracture toughness obtained in tests are representative  $K_{Ic}$  values. Guidelines for the analysis of plane-strain fracture-toughness data and the method of data presentation have been incorporated in Chapter 9 of MIL-HDBK-5B.

Plane-strain fracture toughness,  $K_{Ic}$ , values are presented in the general discussion prefacing each chapter of MIL-HDBK-5B in which data are available. The range and simple average of  $K_{Ic}$  values as well as the number of lots represented by the data are indicated. It is preferable that the data represent a minimum of three specimens each from a minimum of five lots of material for each test direction. Where data are available, the effect of temperature on  $K_{Ic}$  is presented graphically in the "Effect of Temperature" section of each chapter.

Residual Strength - In ductile and thin section structural materials, quasi-plane-strain stress-state conditions may not be achieved due to the lack of third dimensional restraint. Rather, quasi-plane-stress or transitional-stress states may be manifested. In the latter cases, structural elements containing cracks may exhibit significant plastic flow at the crack tip along with some stable crack extension prior to fracture instability. As a result, the characteristic fracture toughness of these material elements may deviate significantly from the plane-strain fracture toughness behavior previously considered. This deviation is reflected in the increasing load-compliance record presented previously in Figure 16.

The stable crack extension prior to fracture associated with this increasing toughness behavior is illustrated schematically in Figure 18. It is quite different from the abrupt elastic fracture which occurs under plane-strain conditions. Two indices of fracture behavior may be associated with this crack growth curve. One is the critical stress-intensity factor,  $K_c$ , determined directly from the instantaneous stress and crack length dimensions at fracture instability, Point C. The other is the apparent stress-intensity factor,  $K_{app}$ , associated with the coordinates of Point N. This latter instance is the residual strength, or apparent toughness concept, of relating the initial crack length to the final fracture stress as a first approximation to the actual crack growth curve. It is the apparent toughness concept that is used in reporting plane-stress and transitional-fracture toughness values in MIL-HDBK-5B.

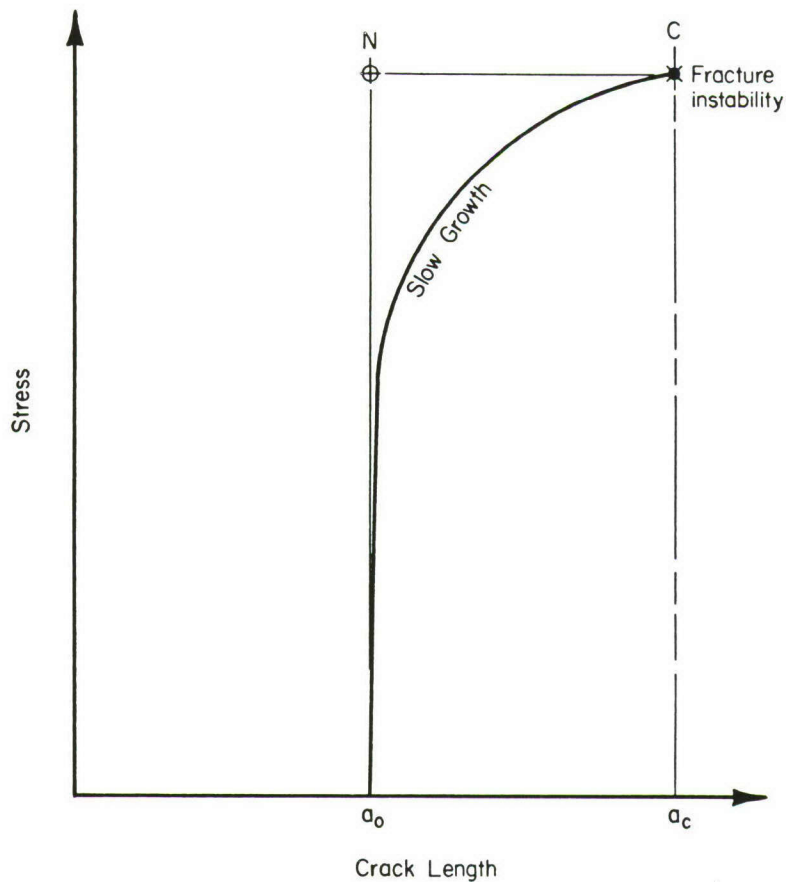


Figure 18. Crack growth curve

Because of the complexity of crack behavior in the plane-stress and transitional-stress states, test methods for evaluating material toughness have not been completely standardized; however, several useful test methods do exist. Although each configuration generates nearly consistent results for that configuration, the results may vary from configuration to configuration. Thus, it is recommended that each general flaw configuration be interpreted and applied within its own design context. Guidelines for the analysis of residual strength data and the method of data presentation was approved at the 46th meeting and will be contained in Chapter 9 of MIL-HDBK-5B in Change Notice 2 revision.

Due to the limited quantity of fracture data available, the fracture-toughness data contained in the Handbook is based upon simple averages and is designated "for information only".

#### STRESS CORROSION

Currently, stress corrosion information is included in MIL-HDBK-5B under "Environmental Considerations" in the "Comments and Properties" section for each alloy, with the exception of the aluminum alloys. When stress corrosion information is included, it is usually a qualitative statement regarding the general stress corrosion resistance of the material. For the aluminum alloys, there is a table which lists values which are an "estimate of highest sustained stress (ksi) at which test specimens of different orientations to the grain structure would not fail in the 3 1/2 percent NaCl alternate immersion test" for the high strength, stress corrosion susceptible materials and tempers.

Because of the increased emphasis on designing to minimize stress corrosion failures, Item 71-4, "Stress Corrosion Threshold Data on Precipitation Hardenable Stainless Steels", was established at the 41st meeting in 1971. The purpose of this item was to determine whether quantitative (threshold)\* data for the precipitation hardening stainless steels could be incorporated into the Handbook.

---

\* A threshold value is defined as the highest sustained stress below which no crack growth nor failure occurs in a certain environment from stress corrosion.

BCL conducted a literature search for applicable stress corrosion data. A review of the literature revealed that due to the lack of a standardized test method for precipitation hardenable stainless steels, available stress corrosion data have been obtained utilizing a variety of test method/specimen design/environment combinations. When similar test conditions were used, testing variables were not uniformly controlled. For these reasons, statistical analyses of existing data were not feasible. Consequently, the incorporation of quantitative stress corrosion data for the precipitation hardenable stainless steels has been deferred until standardized test procedures have been developed.

Currently the ASTM is actively involved in the establishment of standard test practices and methods for stress corrosion testing. The progress of the ASTM in establishing standards has been monitored and reported by BCL personnel at each MIL-HDBK-5 meeting. The ASTM progress will continue to be monitored and reported annually to the MIL-HDBK-5 Coordination Activity until stress corrosion testing standards are published.

Incidental to the investigation of precipitation hardening stainless steel stress corrosion data, it was discovered that there was no description of the methods used for obtaining the stress corrosion data in MIL-HDBK-5 Table 3.1.2.3.1, "Comparison of the Resistance to Stress Corrosion of Various Aluminum Alloys and Products". A section 9.5.1, "Stress-Corrosion Resistance", which specifically describes the test procedure used to obtain the data in Table 3.1.2.3.1 was prepared for incorporation into Chapter 9. This revision was approved at the 44th MIL-HDBK-5 Coordination Meeting on October 25-27, 1972, and will appear in Change Notice 2.

#### CASTING DESIGN DATA

MIL-HDBK-5 Agenda Item 70-1 was originally established to incorporate aluminum casting alloy 201.0 into the handbook on a specification basis. All design allowable properties for casting alloys have been previously presented in the handbook on a specification basis. Some of the reasons for not establishing statistical based allowables in the past were:

- (1) There was a general concern in the aerospace industry and in the government about estimating the properties

in castings from separately cast test bar properties which constituted most of the available data.

- (2) There was the often mentioned aspect of the uniqueness of each casting configuration with its own set of critical or designated areas and associated foundry practice variables.
- (3) There was concern regarding the extent of the variability of properties from casting to casting and from foundry to foundry.

However, with the development of "premium quality" aluminum castings which have mechanical properties approaching those of wrought materials, castings are now being considered for structural applications for economic reasons. This usage in structural applications has resulted in the need for casting design allowables determined on a statistical basis (A and B values).

Since the problems associated with the establishment of A and B values are common to all casting alloys, the scope of the agenda item was modified to include all premium cast aluminum alloys. The objective of the current MIL-HDBK-5 effort is to develop the analytical procedures for determining statistical based design allowable properties for cast materials in MIL-HDBK-5.

Presentations by BCL personnel to the MIL-HDBK-5 Coordination Activity during the past several years have demonstrated several techniques for treating casting data and an overall analytical approach has been developed.

The main questions which have been addressed are:

- (1) How to treat different sizes and shapes of castings?  
The analysis of 29 casting shapes and sizes of one alloy cast at several foundries indicated that major groupings can be made.
- (2) How to treat the many foundry variables such as chills, risers, etc.?

The computer program, AID, can be used to assist in developing a mathematical model for a process. The program can accommodate nonnumeric as well as numeric variables. The nonnumeric variables, as their

importance is identified, can subsequently be incorporated in the analysis by partitioning the data on these variables. Numeric variables can be treated in the usual ways by analysis of given levels of that variable or by regression techniques.

- (3) How do the properties in a casting compare with those obtained from separate cast test bars?

The analysis of data from one foundry over a lengthy production run showed that, in a well-controlled process, integral test bar properties can be related to properties of test bars cut from castings.

The question that remains is: Can sufficient, well-documented data be obtained for a sufficient number of casting configurations and sizes from qualified foundries such that reliable design allowables (A and B values) can be determined?

In order to answer this question, a program plan has been formulated which concentrates on one aluminum alloy, A-357, a widely used casting composition. Although a considerable quantity of casting data has already been received, most of these data lacked documentation of either the foundry variables or the design variables. In addition, it was desirable to extend the data base to include a wider range of casting sizes, configurations, and thicknesses.

The aerospace companies which participate in MIL-HDBK-5 activity have been requested to identify A-357 production castings for which appropriately documented data can be supplied. Concurrently, the aerospace companies will instruct their casting suppliers (foundries) to release the corresponding foundry data for the selected castings.

In addition, an Aluminum Association Task Group on Premium Castings was established in 1973 for the purpose of collecting premium casting mechanical property data which can be used to establish design allowables. These data will be furnished to the MIL-HDBK-5 Coordination Activity for analysis.

All of these data should be received during the first quarter of 1974. If a statistically significant quantity of appropriately documented A-357 data is available, these observations can be used to verify the newly developed analytical procedure for determining design allowables (A and B values) for castings.

## FASTENERS

The level of activity for Chapter 8, "Structural Joints", is best reflected by the activity of the Fastener Task Group. This Group is composed of the following members: T. Dutko, B-1 Division, Rockwell International; W. Vorhes, Vought Aeronautics Company; S. Ford, BCL; W. Hyler, BCL; E. Bateh, Lockheed-Georgia Company; C. Parsons, Boeing Commercial Airplane Company; R. Stewart, ASD, USAF; and A. Cowles, Naval Air Systems Command. The objective of this Group is to review proposals from fastener manufacturers for incorporating new fasteners into the chapter prior to recommending them to the MIL-HDBK-5 Coordination Activity and to provide guidance for those proposals. In addition, this Group is charged with the task of suggesting proposed changes, revisions, or deletions to Chapter 8. A considerable effort is also involved in preparation of revision of fastener guidelines for Chapter 9.

In past years, the method of determining joint yield strength has undergone several changes and for some time rivets and solid shank fasteners were analyzed using different yield criteria. Considerable study by the Fastener Task Group indicated that joint yield strength was excessive for small diameter fasteners. Hence, the Task Group recommended to the Coordination Activity that joint yield load should be a function of fastener diameter and should be determined as the point on the joint load-deflection curve equal to an offset of 4 percent of the fastener diameter. This change was approved and reanalysis of existing data showed that the new criteria provided reduced scatter and less tendency for the data to group together by diameter than previous analytical methods.

Considerable effort has been expended in the revision of Section 9.4.1, "Guidelines for Presentation of Data for Mechanically Fastened Joints". These guidelines provide detailed requirements for data quantity, quality, analysis, and presentation requirements. Additions of specific interest include:

- The new 0.04D yield criteria.
- A method for the analysis of flush-head fasteners whose heads penetrate the second sheet.
- Data requirements and analysis methods for limited quantities of data not intended for inclusion in MIL-HDBK-5.

- Graphical presentation formats and methods of analysis of static joint data.
- Detailed sponsor and reporting requirements for new fasteners.
- A standard failure code.

The final draft of this guideline revision will be presented to the MIL-HDBK-5 Coordination Activity for approval at the 47th meeting on April 23-25, 1974.

The problem of nonstandard hole sizes and fastener shank diameters has received considerable attention. The lack of standardization has made the analysis of fastener proposals extremely difficult in the past. It was decided at the February, 1974 Fastener Task Group meeting, to propose a set of standard shear strength and diameter tables for inclusion in Chapter 8. This proposal will be coordinated with the efforts of the MIL-STD-1515, Aero Mechanical Requirements Group.

A working plan has been devised to implement a complete revision of Chapter 8. This revision will include a complete reanalysis of any of the tables presently in the chapter where adequate load-deflection curves are available. Conjunctively, all tables will be reviewed for content, format, and proper footnotes. The footnotes will indicate the yield-offset used in the data analysis, and, in the case of interference fit fasteners, the interference level. This effort will provide a better basis for comparison of joint data presently published in the document with those items added in the future.

#### REQUIREMENTS FOR NEW MATERIALS

The data requirements and procedure for incorporation of a new material into MIL-HDBK-5B are still apparently unclear to some people. Although this information is currently contained in Section 9.1.6 of MIL-HDBK-5B, these requirements are reiterated in this report because of its widespread distribution. These requirements apply only to new alloys--not fasteners. The data requirements for fasteners are currently being formulated by the Fastener Task Group.

In Change Notice 1 to MIL-HDBK-5B, Section 9.1.6, "Requirements for New Materials", was added to Chapter 9, "Guidelines for the Presentation of

Data". The purpose of Section 9.1.6 was to establish minimum data requirements for new materials to be considered for incorporation into MIL-HDBK-5B. For MIL-HDBK-5 purposes, a new material is one covered by a material specification (MIL, Federal, or AMS), in one product form, in the heat-treat condition or temper and in the thickness range covered by specification. The new alloy may be proposed to the MIL-HDBK-5 Coordination Activity for incorporation into MIL-HDBK-5 on a specification (S) basis with the following required information to be supplied in a report prepared by the organization submitting the proposal.

- (1) A section on "Comments and Properties" should be prepared in a format consistent with the base alloy chapter. This section should provide brief information on metallurgical, manufacturing, and environmental considerations, as well as specifications, heat treatments or tempers and a room temperature table of mechanical and physical properties.
- (2) The following tests are required to provide data for the room temperature property table:
  - (a) At least 10 pairs of tensile and compression data in each significant grain direction for the product form and heat treatment. The 10 pairs of data should encompass the thickness range covered by specification and should be obtained from 5 to 10 different lots or heats of the alloy. These data should be reduced to derived property ratios as described in Section 9.2.9. These ratios are **applied** to the specification tensile values to establish tensile properties in other than material specification test directions and compressive properties in the appropriate grain directions for the product form and thickness.
  - (b) At least three lots or heats, selected from the same group of lots or heats used in (a), should be tested in shear and bearing, to establish derived property

ratios for these properties in a similar manner. These tests also should be conducted in the significant grain directions for the product form.

- (c) From the tests in 2(a), modulus of elasticity in tension and compression should be obtained, preferably precision modulus values. As indicated in Section 9.3.2.2, ASTM E83 Class A extensometers are preferred but Class B extensometers may be used.
  - (d) The room temperature table will be prepared containing  $F_{tu}$ ,  $F_{ty}$ ,  $F_{cy}$ ,  $e$ ,  $E$ , and  $E_c$  values in the significant grain directions over the thickness range considered. The shear and bearing values will also be contained in the table and identified as tentative if based upon less than ten lots or heats. Physical properties  $\omega$ ,  $\alpha$ ,  $C$ , and  $K$  shall be reported in the room temperature table, when available.
- (3) Representative load-strain or stress-strain curves from actual tension and compression tests should be included. Typical (as defined by Section 9.3.2.1) stress-strain curves, preferably full range, including Ramberg-Osgood parameter values as well as compressive tangent modulus curves will be prepared as described in Section 9.3.2 and provided as a portion of the proposed addition to the Handbook.
  - (4) A report shall be submitted to the MIL-HDBK-5 Coordination Activity that contains the proposed addition to the Handbook. The report should include all test data identified by heat or lot, heat treatment, including copies of typical stress-strain curves. The report should contain the specific computations involved in the analysis of derived properties as well as procedures used in the construction of the typical stress-strain curves.
  - (5) Frequently, other testing is done which provides very useful information in the characterization of the material. Such

testing includes: studies of the effect of temperature on various properties, tests to establish optimum heat treatment, stress-corrosion resistance, fracture toughness, and fatigue tests. Inclusion of such data is requested, even though limited in nature.

#### PHYSICAL PROPERTIES

Efforts are currently under way to update the physical properties in MIL-HDBK-5B. A considerable quantity of additional physical property data for some alloys has been generated since the physical property values were incorporated in the Handbook. Agenda item 72-23, Coefficient of Thermal Expansion for Ti-6Al-4V, approved at the 45th meeting, and item 73-8, Physical Property Data for Titanium Alloys, approved at the 46th meeting, have completed the update for the titanium chapter. Agenda item 73-20, Physical Properties of Nickel Base Alloys, is expected to be approved at the 47th meeting in April, 1974. It is planned to present a proposal for one chapter at each meeting until the update of all the physical properties for the various alloys is completed. The method of analyzing and presenting physical property data in MIL-HDBK-5B is described below.

The four physical properties included in MIL-HDBK-5B are density, specific heat, thermal conductivity, and mean coefficient of thermal expansion. Physical properties are presented in MIL-HDBK-5B on a typical basis. The units and symbols employed in MIL-HDBK-5B are tabulated below.

		Symbol	Recommended ASTM test procedures <sup>a</sup>
Density	lb./in. <sup>3</sup>	$\omega$	D-2320
Specific heat	Btu/lb.-F	C	D-2766
Thermal conductivity	Btu/(hr.-ft <sup>2</sup> -F/ft.)	K	C-177, C-518
Mean coefficient of thermal expansion	10 <sup>-6</sup> (in./in./F)	$\alpha$	E228, E289

<sup>a</sup>These procedures are not now included in MIL-HDBK-5B, but will be recommended for approval and should appear in the next change notice revision.

These four properties are presented in the room temperature property tables as typical values. Effect of temperature data may be available for

specific heat, thermal conductivity, or thermal expansion in which case they are presented graphically instead. The three properties are shown in a single figure, each property being represented by a best-fit smooth curve drawn through the typical values at each temperature.

The analysis and presentation procedures are illustrated by the following working curves and summary figure from a recent MIL-HDBK-5 agenda item, 73-8, on physical property data for the titanium chapter.

The Thermalphysical Properties Research Center (TPRC) is considered the primary reference authority for physical property data to be included in MIL-HDBK-5B, but data from many other sources are also utilized. A variety of units are used to report thermophysical property data in the literature so that after collection, the data are converted to MIL-HDBK-5 units and plotted in working curves. Figures 19 through 21 show data from multiple sources plotted for each of the three thermal physical properties. Earlier MIL-HDBK-5B curves based on a single source are presented for comparison. For mean thermal expansion, Figure 22, the reference temperature is indicated on the figure. This is an approved procedure that is not yet reflected in the Chapter 9 guidelines, but will be included in the next change notice. When data over a wide temperature range, as in Figures 19 and 21, are available, the overall curve shape is more accurately determined, even though the design temperature range in the MIL-HDBK-5B illustration, Figure 22, may be more limited. The MIL-HDBK-5 design curve reports the basis for each of the three properties. The references used in the determination of physical properties are included in the agenda proposal. References (24) through (27) were used in commercially pure titanium items.

- 
- (24) Touloukian, Y. S., editor, "Thermophysical Properties of High Temperature Solid Material", Volume 2, Parts I and II, Purdue University (1967), and Touloukian, Y. S., Powell, R. W., Ho, C. Y., and Klemens, P. G., "Thermophysical Properties of Matter, Volumes 1 and 4, Purdue University (1970).
  - (25) "Aerospace Structural Metals Handbook", AFML-TR-68-115, Mechanical Properties Data Center, Belfour Stulen, Inc. (1973).
  - (26) "Metals Handbook, Vol. 1, Properties and Selection of Metals", 8th Edition, American Society for Metals (1961).
  - (27) "Rem-Cru A-40, A-55, and A-70", Rem-Cru Titanium Data Sheet, Rem-Cru Titanium, Inc. (February, 1956).

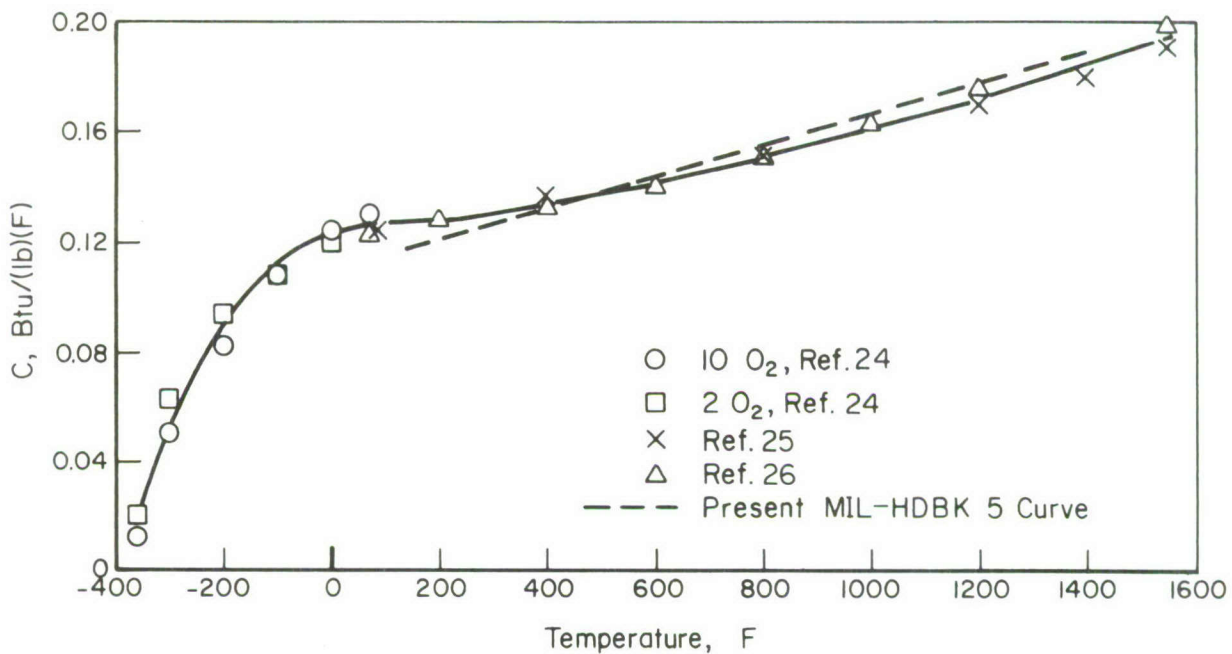


Figure 19. Working curve showing effect of temperature on the specific heat of commercially pure titanium.

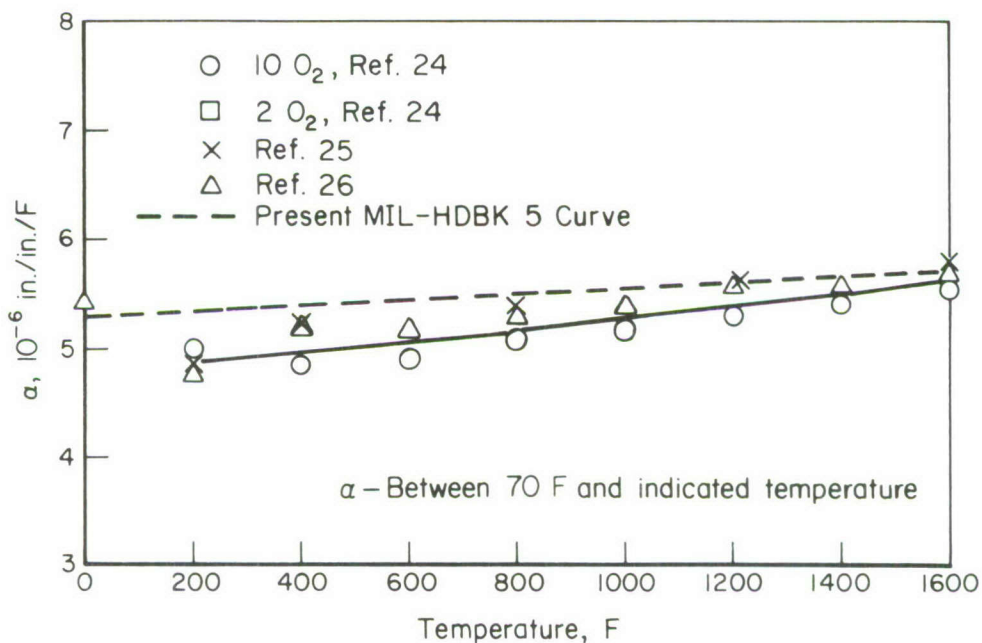


Figure 20. Working curve showing effect of temperature on the thermal expansion of commercially pure titanium.

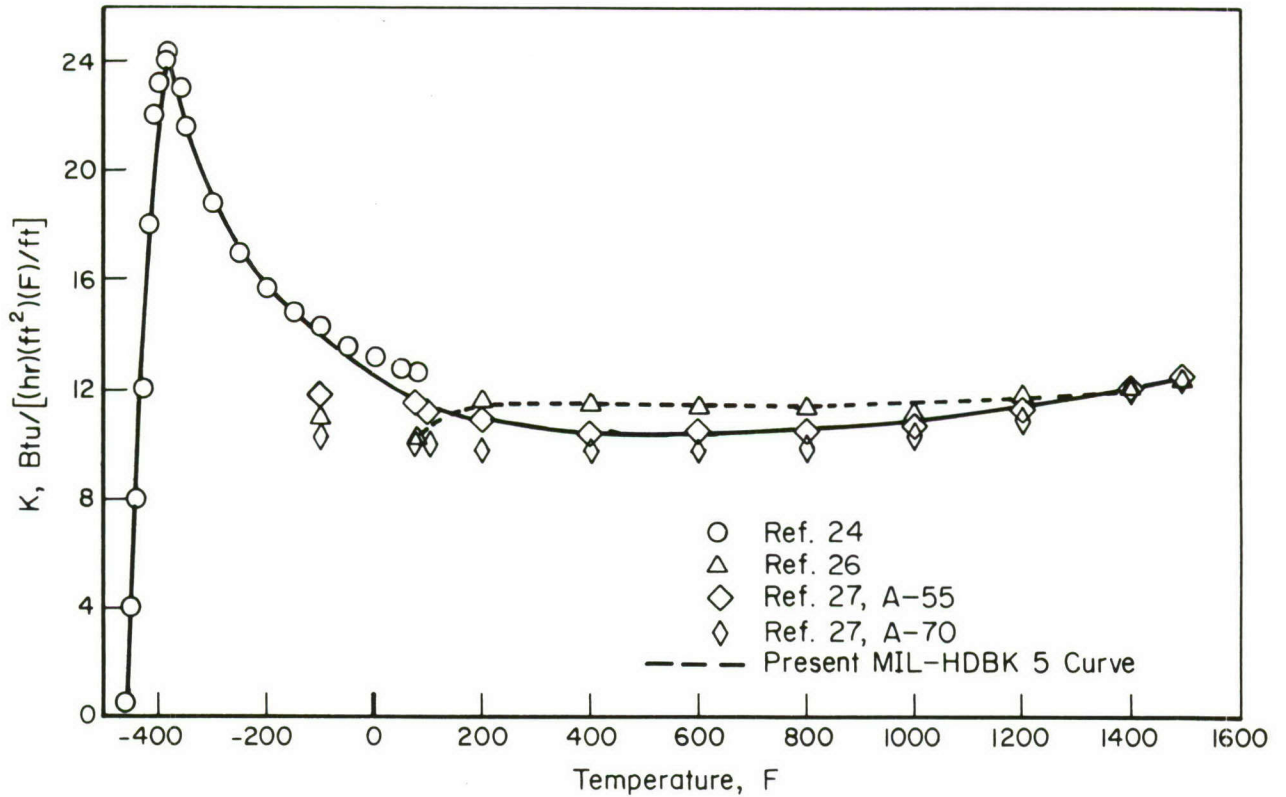


Figure 21. Working curve showing effect of temperature on the thermal conductivity of commercially pure titanium.

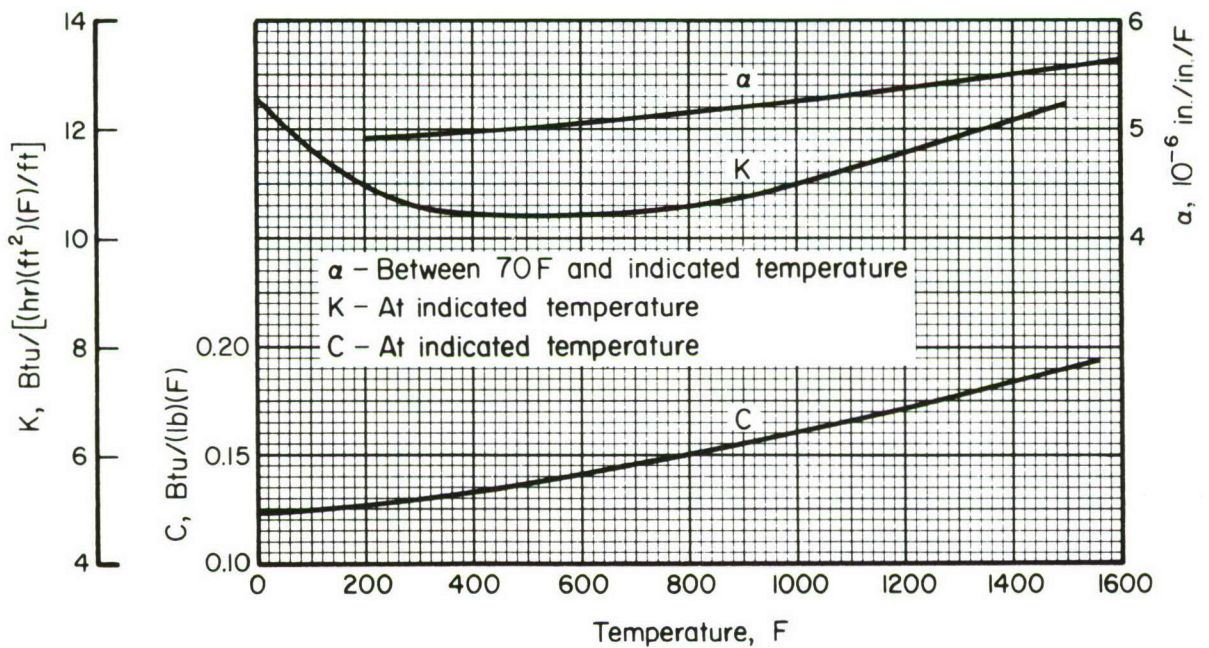


Figure 22. Effect of temperature on the physical properties of commercially pure titanium (MIL-HDBK-5 Figure 5.2.1.0).

## STRESS-STRAIN AND STRESS-TANGENT MODULUS CURVES

At the 43rd MIL-HDBK-5 Meeting, a study (Agenda Item 70-21) to determine what type of stress-strain curves (typical or minimum) and tangent-modulus curves should be presented in MIL-HDBK-5B was concluded. From the results of that investigation it was determined that:

- (1) All stress-strain curves (for tension, compression, and tangent modulus) should continue to be presented on a "typical" basis. The curves preferably should be full-range and prominently marked "Typical".
- (2) The graph showing typical compression stress-strain curves should also contain the corresponding compression tangent-modulus curves.
- (3) Tension tangent-modulus curves should be deleted from MIL-HDBK-5B and will no longer be included.
- (4) The Ramberg-Osgood  $n$  exponent should appear on the graphs.

Accordingly, the guidelines, Section 9.3.2, "Typical Stress-Strain and Stress-Tangent Modulus Curves", was revised to include the above requirements and incorporated in the Change Notice 1 revision. This new revision also contained the Ramberg-Osgood method for determining stress-strain curves. This procedure is an alternative to the strain-departure technique.

The establishment of these new requirements for stress-strain curves necessitated the updating of existing stress-strain curves in the Handbook. A considerable number of curves were updated in Change Notices 1 and 2, and this task will continue until completed.

In addition, more emphasis has been placed on the incorporation of stress-strain curves in the Document. As an example, Alcoa submitted 49 sets of typical stress-strain curves for various aluminum alloy products (Agenda Item 72-6) now contained in the Handbook. Some of the curves were for new alloys or tempers while others updated existing curves. From these data, stress-strain curves were prepared in accordance with the revised guidelines by BCL personnel. These curves will appear in Change Notice 2 revision.

### Preparation of Stress-Strain Curves

The mechanics involved in the construction of stress-strain curves are described below. The tension and compression stress-strain curves

appearing in MIL-HDBK-5B are described as "typical" but are in reality constructed curves. The term "typical", in this case, indicates that representative stress-strain data have been adjusted.

The first adjustment is the use of the room temperature tabulated elastic modulus value for the material or the computed elastic modulus at the appropriate temperature. The computation of modulus at temperature is made by multiplying the room temperature modulus by the percentage from the curve depicting percent of room temperature modulus as a function of temperature.

A second adjustment involves a displacement of the plastic portions of the stress-strain curve so that it passes through the average (or typical) value of 0.2 percent yield strength for that product. The typical Ramberg-Osgood parameter as determined from representative stress-strain curves is used to determine shape factors in plastic region. Thus, the preparation of each stress-strain curve requires (1) representative original stress-strain curves to obtain typical Ramberg-Osgood parameter, (2) product-average values for the yield strength and elastic modulus at test temperature. After preparation, the constructed stress-strain curve is compared with original curves to check the shape. Examples of recently proposed stress-strain curves for MIL-HDBK-5B are shown in Figures 23 through 25.

Figure 23 shows typical tensile stress-strain curves for 15-5PH steel at room temperature. These curves show a common modulus which this material exhibits for various heat treated conditions.

Figure 24 depicts typical tensile stress-strain curves for Inconel Alloy 625 at room and elevated temperatures. In this case, the moduli were determined from the tabulated modulus at room temperature and the computed values from the effect of temperature on modulus curves. The curves pass through the average 0.2 percent yield strengths at each temperature.

Figure 25 shows typical compressive stress-strain curves for Inconel Alloy 625. The compressive tangent modulus curves are presented on the same figure with the compression stress-strain curve.

On all figures the Ramberg-Osgood parameters are listed and the word "typical" is displayed on the graph as well as in the title.

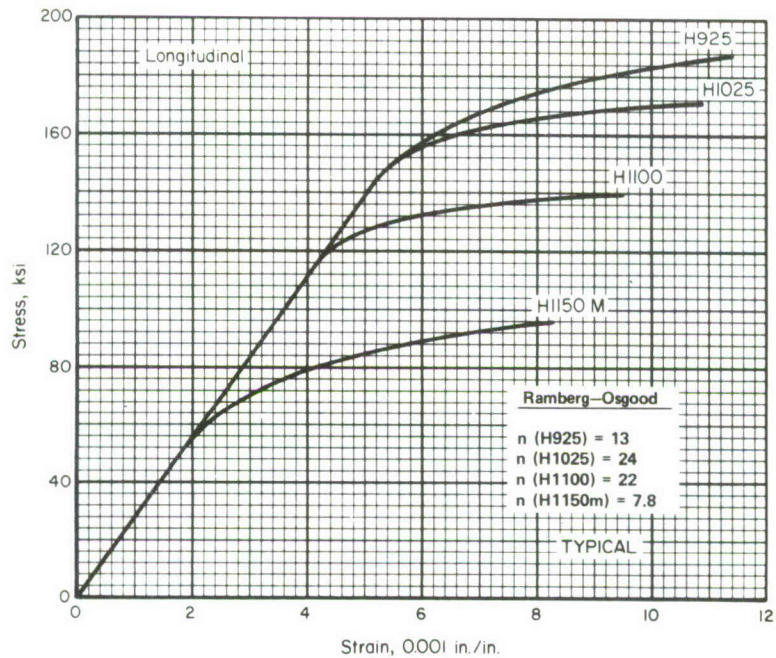


Figure 23. Typical tensile stress-strain curves at room temperature for various heat treated conditions of 15-5PH stainless steel bar.

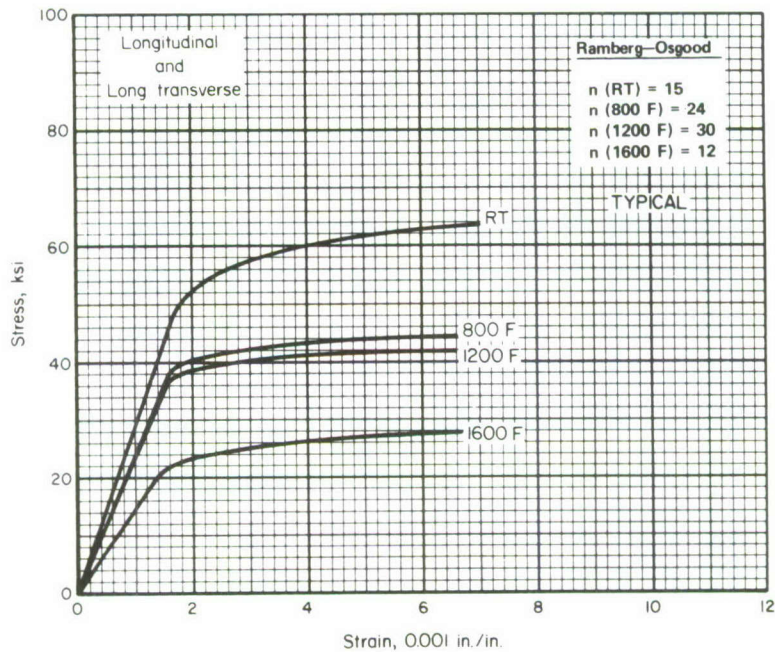


Figure 24. Typical tensile stress-strain curves for annealed Inconel Alloy 625 sheet at room and elevated temperatures.

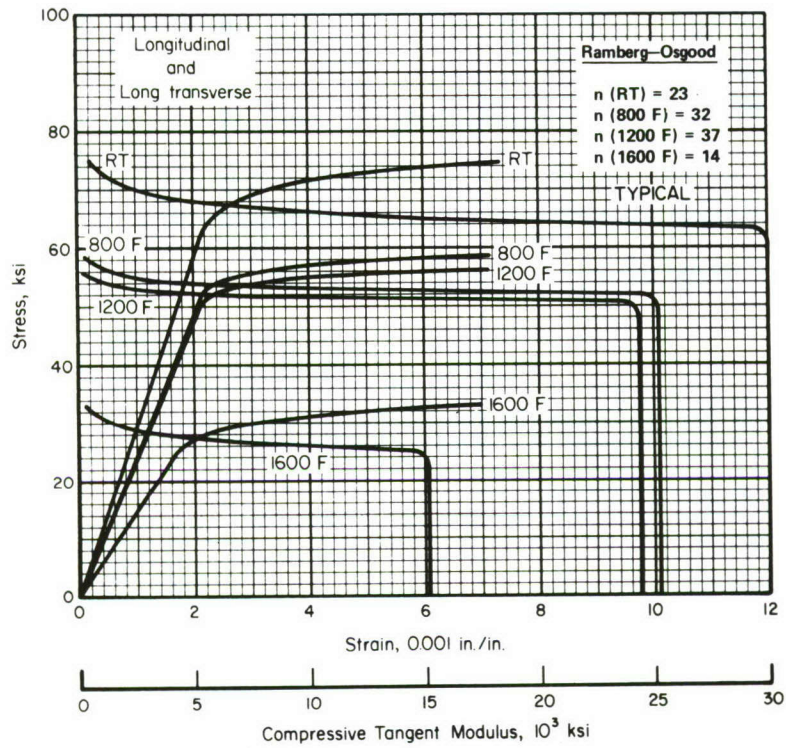


Figure 25. Typical compressive stress-strain and tangent modulus curves for annealed Inconel Alloy 625 sheet at room and elevated temperatures.

## MIL-HDBK-5B REVISIONS

One change notice to MIL-HDBK-5B has been issued and another is pending. Change Notice 1, dated July 1, 1972, which incorporated the changes and additions approved at the 42nd and 43rd meetings, was issued in February, 1973. Change Notice 2, dated August 31, 1973, which included the changes and additions approved at the 44th and 45th meetings, is in the process of being printed and should be available in May, 1974. It is planned to issue only one more change notice covering approvals at the 46th and 47th meetings before publishing a complete revision of MIL-HDBK-5.

## MIL-HDBK-5 TEST PROGRAM

During the reporting period, the Army Materials and Mechanics Research Center provided funds for a test program. The objective of this test program was to perform the necessary tests required to provide missing design properties in MIL-HDBK-5B. After a complete review of MIL-HDBK-5B to identify missing data, five alloys were selected for testing. The literature was searched for data pertinent to the missing properties. Taking into consideration available data from the literature, test programs were designed for the five alloys to acquire sufficient data so that certain missing design allowables can be determined. The following tests will be conducted on the five selected materials:

- (1) 9Ni-Co-.20C Plate -  
Room and elevated temperature tensile, compression and shear
- (2) Ti-6Al-6V-2Sn Extrusion -  
Room temperature tensile, shear, and bearing  
Elevated temperature tensile, compression and shear
- (3) 17-4PH Bar -  
Room temperature tensile, compression and shear for H1025 and H1150 conditions
- (4) 15-5PH Bar -  
Room temperature tensile, compression, shear, and bearing for H1025 condition  
Room temperature tensile, compression and shear for H1150 condition

(5) 2024-T86 Sheet -

Room temperature tension and compression tests after exposure to 300, 350, 400, and 450 F for 1, 10, 100, and 1000 hours.

Tensile and shear tests for 17-4PH and 15-5PH have been completed. After completion of the testing, the data from the literature and the test data will be statistically analyzed to determine the missing design properties.

## APPENDIX A

### STATISTICAL METHODS OF ANALYSIS

The phenomenological approach to the study of fatigue is usually concerned with formulating a model of material behavior. In the present program, this model took the form of a regression equation that was fitted to empirical data. Statistical analysis provided a method by which the performance of the various empirical models could be compared and evaluated. The formulations which were used in the analysis are discussed in the following section.

In the fatigue analysis, a third-order polynomial proved to be useful for many of the initial comparative studies. The equation was written in the following form:

$$\log N_f = B_1 + B_2 \epsilon_{eq} + B_3 \epsilon_{eq}^2 + B_4 \epsilon_{eq}^3 \quad . \quad (A1)$$

Further investigations revealed that Equation (A1) could be simplified to a linear regression equation involving a single independent variable,

$$Y = A_0 + A_1 X \quad , \quad (A2)$$

where X represented a mapping function linearly related to the dependent variable Y.\* A least-squares regression procedure was used to establish optimum coefficients for Equations (A1) and (A2). The optimization procedure was based on a minimization of the standard error of estimate.

$$s = \sqrt{\frac{\sum(Y-\bar{Y})^2}{n-2}} \quad . \quad (A3)$$

Different formulations for the independent variables were compared through calculation of the statistical parameter,  $R^2$ . This factor, which provided a quantitative estimate of goodness of fit, was used to describe the fraction of the sum of squares of deviations of the dependent variable from its mean associated with the regression. It was defined by the relationship

$$R^2 = 1 - \text{SSD}/\text{TSS} = 1 - \frac{\sum(Y_i - \bar{Y})^2}{\sum Y^2} \quad . \quad (A4)$$

---

\* The exact definition of this mapping function was omitted here for simplicity; it is defined in Equation (9) of the text.

Values of  $R^2$  approaching 100 percent were considered most desirable, since that tendency indicated a large percentage of the variance of the dependent variable was attributable to the regression. In the case of fatigue, such values of  $R^2$  indicated a good correlation between equivalent strain and fatigue life.

After screening the formulations of interest, it was considered desirable to establish tolerance limits on the best empirical models. These tolerance limits were calculated to define an interval which can be claimed to contain a specified proportion of the data population with a specific degree of confidence. Before tolerance limits could be calculated, it was necessary to determine whether the data satisfied the appropriate statistical conditions. Primarily, the data had to be independent and be normally distributed about the regression line and had to have zero mean deviations from that line and have a constant variance<sup>(28)</sup>.

When the residuals (or deviations from the mean curve) were plotted as a function of actual values of the dependent variable, it was possible to determine, by inspection, whether the data were independent and had an essentially uniform variance throughout their range. Actual values for the dependent variable were used since it was then possible to compare different fitting functions without changing the fatigue life values of individual data points on the residual plot. If only one fitting function had been studied, it would have been reasonable to use predicted values of the dependent variable as is customary in most statistical analyses. The additional criterion of log-normality was tested in several cases through construction and examination of frequency distribution plots of the residuals. Although log-normality of the data was not proved, the frequency distribution plots indicated that the data were not skewed appreciably and were reasonably approximated by a log-normal distribution.

After statistical conditions were satisfied, it was possible to calculate the estimated variance of a specific value of Y about the regression line. For a first order equation [Equation (A2)], the point estimate of variance was defined according to the following expression:

---

(28) Draper, N. R., and Smith, H., Applied Regression Analysis, Wiley Publications in Statistics (1966).

$$V = s^2 \left[ \frac{1}{n} + \frac{(X - \bar{X})^2}{\sum (X_i - \bar{X}_i)^2} \right] \quad . \quad (A5)$$

To solve Equation (A5), it was necessary to determine values of  $X_i$  for each data value based on values of  $\epsilon_{eq}$ . Then  $\bar{X}$  was calculated as a simple average of the  $X_i$ 's. The same process was used in order to calculate  $s^2$ , based on values of  $Y_i$ . After these calculations were completed, the variance was calculated for a selected value of  $X$ . Knowing the estimates of variance at  $X$ , it was then possible to determine tolerance limits of level ( $u$ ) at a desired confidence ( $v$ ), according to the following formulation<sup>(29)</sup>:

$$Y_{u,v} = Y \pm t \sqrt{s^2 + V} \quad . \quad (A6)$$

---

(29) Williams, E. J., Regression Analysis, Wiley Publications in Statistics (1959).

## REFERENCES

- (1) Ruff, Paul E., Favor, Ronald J., and Hyler, Walter S., "The Collection, Generation, and Analysis of MIL-HDBK-5 Allowable Design Data", AFML-TR-72-61 (March, 1972).
- (2) Ruff, Paul E., Favor, Ronald J., and Hyler, Walter S., "The Collection, Generation, and Analysis of MIL-HDBK-5 Allowable Design Data", AFML-TR-73-79 (March, 1973).
- (3) Jaske, C. E., Feddersen, C. E., Davies, K. B., and Rice, R. C., "Analysis of Fatigue, Fatigue-Crack Propagation, and Fracture Data", Final Report to NASA-Langley Research Center, NASA CR-132332 (November, 1973).
- (4) Rice, R. C., and Jaske, C. E., "Consolidated Presentation of Fatigue Data for Design Applications", presented at the 1974 SAE Automotive Engineering Congress and Exposition, Detroit, Michigan (February, 1974).
- (5) Walker, K., "The Effect of Stress Ratio During Crack Propagation and Fatigue for 2024-T3 and 7075-T6 Aluminum", Effects of Environment and Complex Load History on Fatigue Life, STP 462, ASTM (1970), pp 1-14.
- (6) Metal Fatigue, Edited by G. Sines and J. L. Waisman, McGraw-Hill Book Company (1959), "Notch-Sensitivity" (R. E. Peterson), pp 293-306.
- (7) Grover, H. J., Bishop, S. M., and Jackson, L. R., "Fatigue Strength of Aircraft Materials Axial-Load Fatigue Tests on Unnotched Sheet Specimens of 24S-T3 and 75S-T6 Aluminum Alloys and of SAE 4130 Steel", NACA TN 2324 (1951).
- (8) Illg, W., "Fatigue Tests on Notched and Unnotched Sheet Specimens of 2024-T3 and 7075-T6 Aluminum Alloys and of SAE 4130 Steel with Special Consideration of the Life Range from 2 to 10,000 Cycles", NACA TN 3866 (1959).
- (9) Grover, H. J., Bishop, S. M., and Jackson, L. R., "Fatigue Strengths of Aircraft Materials Axial-Load Fatigue Tests on Notched Sheet Specimens of 24S-T3 and 75S-T6 Aluminum Alloys and of SAE 4130 Steel with Stress-Concentration Factors of 2.0 and 4.0", NACA TN 2389 (1951).
- (10) Grover, H. J., Bishop, S. M., and Jackson, L. R., "Fatigue Strengths of Aircraft Materials Axial-Load Fatigue Tests on Notched Sheet Specimens of 24S-T3 and 75S-T6 Aluminum Alloys and of SAE 4130 Steel with Stress-Concentration Factor of 5.0", NACA TN 2390 (1951).
- (11) Grover, H. J., Hyler, W. S., and Jackson, L. R., "Fatigue Strengths of Aircraft Materials Axial-Load Fatigue Tests on Notched Sheet Specimens of 24S-T3 and 75S-T6 Aluminum Alloys and SAE 4130 Steel with Stress-Concentration Factor of 1.5", NACA TN 2639 (1952).

- (12) Hardrath, H. F., and Illg, W., "Fatigue Tests at Stresses Producing Failure in 2 to 10,000 Cycles, 24S-T3 and 75S-T6 Aluminum Alloy Sheet Specimens with a Theoretical Stress-Concentration Factor of 4.0 Subjected to Completely Reversed Axial Load", NACA TN 3132 (1954).
- (13) Landers, C. B., and Hardrath, H. F., "Results of Axial-Load Fatigue Tests on Electropolished 2024-T3 and 7075-T6 Aluminum Alloy Sheet Specimens with Central Holes", NACA TN 3631 (1956).
- (14) Grover, H. J., Hyler, W. S., and Jackson, L. R., "Fatigue Strengths of Aircraft Materials Axial-Load Fatigue Tests in Edge-Notched Sheet Specimens of 2024-T3 and 7075-T6 Aluminum Alloys and of SAE 4130 Steel with Notch Radii of 0.004 and 0.070 Inch", NASA TN D-111 (1959).
- (15) Naumann, E. C., Hardrath, H. F., and Guthrie, D. E., "Axial-Load Fatigue Tests of 2024-T3 and 7075-T6 Aluminum Alloys and of SAE 4130 Steel with Notch Radii of 0.004 and 0.070 Inch", NASA TN D-111 (1959).
- (16) Smith, C. R., "S-N Characteristics of Notched Specimens", NASA CR-54503 (1966).
- (17) Bateh, E. J., and McGee, W., "Axial Load Fatigue and Tensile Properties of 300 VAR Steel Heat Treated to 280-300 ksi", ER-10202 (MCIC 74342), Lockheed-Georgia Company (1969).
- (18) Harmsworth, C. L., "Low-Cycle Fatigue Evaluation of Titanium 6Al-6V-2Sn and 300M Steel for Landing Gear Applications", AFML-TR-69-48 (1969).
- (19) Deel, O. L., and Mindlin, H., "Engineering Data on New and Emerging Structural Materials", AFML-TR-70-252 (1970).
- (20) Jaske, C. E., "The Influence of Chemical Milling on Fatigue Behavior of 300M VAR Steel", Final Report (April, 1969).
- (21) Jaske, C. E., "The Influence of Variation in Decarburization Level Upon Fatigue Life of 300M VAR Steel", Letter Report to the Bendix Corporation (September 30, 1968).
- (22) Anon., "Determination of Design Data for Heat Treated Titanium Alloy Sheet", Vol. 3 - Tables of Data Collected, ASD-TDR-335, Lockheed-Georgia Company (1962).
- (23) Collipriest, J. E., "An Experimentalist's View of the Surface Flaw Problem", The Surface Crack: Physical Problems and Computational Solutions, ASME, New York (1972), pp 43-62.
- (24) Touloukian, Y. S., editor, "Thermophysical Properties of High Temperature Solid Material", Volume 2, Parts I and II, Purdue University (1967), and Touloukian, Y. S., Powell, R. W., Ho, C. Y., and Klemens, P. G., "Thermophysical Properties of Matter, Volumes 1 and 4, Purdue University (1970).

- (25) "Aerospace Structural Metals Handbook", AFML-TR-68-115, Mechanical Properties Data Center, Belfour Stulen, Inc. (1973).
- (26) "Metals Handbook, Vol. 1, Properties and Selection of Metals", 8th Edition, American Society for Metals (1961).
- (27) "Rem-Cru A-40, A-55, and A-70", Rem-Cru Titanium Data Sheet, Rem-Cru Titanium, Inc. (February, 1956).
- (28) Draper, N. R., and Smith, H., Applied Regression Analysis, Wiley Publications in Statistics (1966).
- (29) Williams, E. J., Regression Analysis, Wiley Publications in Statistics (1959).

## SYMBOLS

a	instantaneous crack size, crack size
$A_0, A_1, A_2, A_3$	regression coefficients
C	specific heat
$C_1, C_2$	regression derived coefficients
E	elastic tension modulus, $\text{MN/m}^2$ (ksi)
$E_c$	elastic compression modulus
e	elongation in percent
$e_a$	nominal strain range
F	stress applied to the cross section
$F_{cy}$	compressive yield strength design allowable
$F_{tu}$	ultimate tensile strength design allowable
$F_{ty}$	tensile yield strength design allowable
K	stress intensity factor, thermal conductivity
$K_c$	plane-stress critical fracture toughness
$K_{Ic}$	plane-strain fracture toughness
$K_f$	fatigue strength reduction factor
$K_o$	crack propagation threshold stress intensity factor
$K_{max}$	maximum cyclic stress intensity factor
$K_t$	theoretical stress concentration factor
$K_e$	strain concentration factor
$K_\sigma$	stress concentration factor
$K_1, K_2$	strength coefficients, $\text{MN/m}^2$ (ksi)
$\Delta K$	range of cyclic stress intensity factor
k	Stulen coefficient
m	Walker exponent, coupling exponent

$N_f$	number of cycles to failure
$n_1, n_2$	strain hardening exponents
$r$	notch root radius, mm (in.)
$R$	stress ratio
$R^2$	proportion of variation explained by regression equation
$R_m^2$	modification of $R^2$ to account for degrees of freedom and sample size
$\Delta S$	cyclic stress range
$S_{max}$	maximum nominal stress, MN/m <sup>2</sup> (ksi)
$S_{min}$	minimum nominal stress
$s$	standard error of estimate
$t$	Students' t multiplier
$u$	confidence level
$V$	point estimate of variance
$W(\epsilon_{eq})$	equivalent strain weighting function
$X$	independent variable - $\tanh^{-1}[\Phi(\epsilon_{eq})]$
$X_i$	ith value of independent variable
$\bar{X}$	mean value of X
$Y$	dependent variable - log N, nondimensional geometric factor scaling crack size with structural size
$Y_i$	ith value of dependent variable
$\bar{Y}$	mean value of Y
$Y_{u,v}$	tolerance limit at a level of confidence (u) for a given number of degrees of freedom (v)
$\alpha$	mean stress exponent, mean coefficient of thermal expansion
$\epsilon_a$	local strain amplitude
$\epsilon_a'$	local strain amplitude based on monotonic stress-strain parameters

$\epsilon_e$	lower limit of inverse hyperbolic tangent function
$\epsilon_{eq}$	equivalent local strain
$\epsilon_u$	upper limit of inverse hyperbolic tangent function
$\nu$	degrees of freedom
$\rho$	notch analysis material constant
$\sigma_a$	local stress amplitude, MN/m <sup>2</sup> (ksi)
$\sigma_a'$	local stress amplitude based on monotonic stress-strain parameters, MN/m <sup>2</sup> (ksi)
$\sigma_a(1), \sigma_a(2)$	specific values of $\sigma_a$ used to define stress-strain curve
$\sigma_m$	mean local stress, MN/m <sup>2</sup> (ksi)
$\sigma_{max}$	maximum local stress, MN/m <sup>2</sup> (ksi)
$\Phi(\epsilon_{eq})$	equivalent strain scaling function
$\omega$	density